New Spatiotemporal Phenomena in Cancer-Host Interactions and Tumor Functional Border Definition via Electrical Impedance Dynamics

Yuri F. Babich

Abstract. The Hanahan-Weinberg criteria interpret cancer as an ecosystem that evolves as a complex adaptive subsystem within a larger open human system. The original technology of functional imaging "The Skin Electrodynamic Introscopy" enabled discovery of previously unknown phenomena of spatial reorganization of the spectral electrical impedance landscape (SEL) in the melanoma area: significant excess of the impedance boundaries of the tumor compared to the visible ones, emergence of autowave and antiphase structures in response to mild stimuli such as short ischemia and non-thermal EMF.

This work aimed at biological understanding of these self-organisation phenomena based on more thorough processing and analysing data of 5 experiments with the aid methods of correlation and fluctuation fields, difference images and graphical analysis. A whole range of new phenomena and effects have been additionally identified. Most of them were contextualized within the "Order from chaos" concept of theory of dissipative structures (DS):

- Emergence and relaxation of DS;
- Emergence of antiphase structure as a marker of the tumor invasive front,
- Temporary expansion of the tumor impedance boundaries in response to the stimuli;
- Transition from initially chaotic SEL to the tumor specific patterns and back upon cessation of the stimulus;
- Cyclic discrete transitions between two dynamical regimes of spatial correlation in the rhythm of the applied stimuli;
- Manifestation of stroma of pre-existing nevus at the mitochondrial fluctuation field;
- Emergence of the tumor resistance zone to the influence as a direct (post) effect of cancer-host interaction;
- Ionic imbalance patterning etc.

The phenomena of self-organization and DS are fundamentally based on mechanisms of intercellular communication. It was shown that when these mechanisms undergo complete destruction through X-rays therapy, these phenomena were either significantly weakened or completely lost. From the point of view of the DS theory, the revealed impedance boundaries of the tumor can be interpreted as an effective zone of entropy/negentropy flow from the tumor. Respectively, the functional boundaries of the tumor can be assessed by the initial impedance boundaries and their progression caused by stimulation of the entropy flow. It is also appropriate to recall that, in contrast to the electrodynamics of individual cells, the phenomena presented reflect the average collective electrodynamics of multi-thousand cell ensembles underlying self-organization processes.

The results demonstrate the potential of dynamic electrical impedance imaging to delineate tumor heterogeneity, define its functional boundaries, and evaluate cancer-host interactions during targeted interventions in real time.

Key words: tumor, melanoma, boundary, dynamic imaging, electrical impedance, coherence, dissipative structures, entropy, EMF, MF.

Introduction

If the entropy changes at the border of the tumorous and the normal tissues are compared as cancers' velocity, then the ratio between the two forms of tissue may be characteristic of the borderline, where an overlap in entropy production rate may be found between the normal tissues and the tumor. This can be considered a new target for demarcation". I. Prigogine[1]

Although tremendous progress medical technologies has been achieved in the 21st century, early diagnosis and complete recovery of malignant tumors are still facing severe challenges: cancer remains a dominating health concern around the world. At the same time, research into cancer initiation and progression has been overwhelmingly directed towards the biochemistry, genomics, and cell biology of cancer. By contrast, far less attention has been focused on the biophysics and system biology of the cancer state[2]. Description of order and function in biological systems has been a challenge to scientists for many decades. The overwhelming majority of biological order is functional order, often representing self-organized dynamical states in living matter[3]. Systems biology has emerged as a powerful paradigm in the life sciences. It is based on the assumption that the properties of complex systems consisting of many components interacting with each other in a nonlinear, nonadditive manner cannot be understood by focusing only on the components. The system as a whole has emergent properties that *are not visible at the level of its parts but o*nly at the *macro view*[4]. The process of self-organisation is often triggered by *seemingly random fluctuations*, amplified by positive feedback. Examples include crystallization, cyclones, Zhabotinsky reactions, all living matter. Ecological examples presupposes spatial and functional differentiation like bacteria and ant colonies, flocking behaviour etc.

The Hanahan-Weinberg hallmarks demonstrate cancer is an ecosystem, which evolves as complex adaptive subsystem within a larger open human system: a neoplasm is formed on the site and from parts of a previous system, which found itself at a bifurcation point[5].

The physics of this phenomenon is based on the theory of dissipative structures (DS), a concept introduced by Ilya Prigogine, a Nobel laureate in chemistry, to describe systems that maintain themselves in a state far from equilibrium by dissipating energy. DS are characterized by their ability to exchange matter, energy, and information with their environment to sustain their existence, they occur when a steady state becomes unstable at a critical bifurcation point[6]. DS exist at all scales, systems, and at different levels of complexity: from the universe to quantum mechanics[7,8]. Recent research into bio-analogue dissipative electrically and chemically driven systems revealed that some of these structures exhibit organism-like behavior, reinforcing the earlier expectation that the study of DS will provide insights into the nature of organisms and their origin[9-11].

The assessment of tumor boundaries is a critical component in the diagnosis, treatment planning, and monitoring of cancer progression. Traditional methods for delineating tumor margins often rely on static imaging techniques such as MRI or CT scans, which may not provide an accurate representation of the tumor's dynamic behavior or its interaction with the surrounding tissues. This limitation underscores the need for innovative approaches that can visualize and monitor tumor boundaries in real time, both in vivo and in vitro. By identifying regions where healthy tissue interacts with tumor cells, researchers can explore novel treatment strategies aimed at disrupting these interactions or restoring normal tissue function[12].

There are few references in the literature to in vivo tissue studies on visualization of DS effects at tissue level. To distinguish malignancy from benignity, current clinical and laboratory methods primarily rely on classical thermodynamics of equilibrium processes (volume, temperature, pressure) rather than nonequilibrium ones[13]. Common methods for tracing dissipative self-assembly, such as dynamic light scattering, electron microscopy, and rheological methods, have some drawbacks, including signal delay, low sensitivity, and low spatial and temporal resolution. The fluorescence method is more popular due to its low cost, ease of use, high sensitivity, and real-time monitoring capabilities[14]. However, it also has some known limitations: dependence on probes, quenching, and potential damage from both light exposure and the fluorophores themselves. Given the dynamic nature of dissipative structures, their direct visualization and real-time monitoring are highly desirable as they can provide 'movies' rather than merely 'snapshots,' offering a better understanding of the kinetic aspects[15].

All physiological phenomena, specifically communicational, directly or indirectly, are inherently bioelectrical[16]. Therefore, electrical impedance spectroscopy (EIS) appears to be particularly promising and, in recent decades, became already established technique in both in vivo and in vitro cancer studies. In general, the advantages of electrical methods for studying information processes, including intercellular interactions, are their ability to provide real-time data with high resolution, sensitivity to subtle changes, and non-invasiveness when applied to intact biological systems[17].

Electrometric methods in general and electrical impedance ones in particular, has become a powerful tool, allowing for rapid, non-invasive, and label-free acquisition of electrical parameters of single cells[18]. These studies have long been a mainstay of cancer research, providing controlled environments to observe cell behavior. However, these models often fail to replicate the complexity of living tissue. The limitations inherent in two-dimensional cell cultures or even three-dimensional spheroids highlight the necessity for more representative models and technique that can capture the dynamic interplay between cancer cells and their microenvironment. However, the existing in vivo EIS has largely remained a static method that does not provide real-time visualizations. To study heterogeneous dynamic structures in biological tissue, it is essential to incorporate adequate spatial and temporal resolution into time-lapse impedance assays. Conventional EIS have only partially bridged the gap between the macro- and microscale measurements: its temporal resolution remains in the range of several minutes, rendering it unsuitable for imaging metabolic landscape with rapidly changing properties[19-23]. Thus, the delineation of real tumor boundaries is a common problem for

all methods, like optical or conventional EIS, based on assessment of the tissue stationary features. Due to the lack of objective criteria, surgeons follow unfounded instructions to make indentations from the visible borders of melanoma, risking both removing healthy tissue and leaving malignant one.

The concept of negentropy/information flow between cancer and healthy cells is an intriguing topic of research in cancer biology. Recent discoveries suggest that tumors may exhibit self-organizing properties influenced by their surroundings. This concept posits that as tumor cells proliferate, they create gradients of biochemical signals and mechanical forces that shape their local environment. These gradients can lead to distinct functional boundaries around tumors—areas where cellular behavior transitions from normal to malignant[24,25].

It has been established that the rate of entropy production of cancer cells is always higher than that of healthy cells, but there is one interesting exception: provided that no external field is applied to them. When an external force field like magnetic (MF) and electromagnetic fields (EMF) is applied, the rate of entropy production of normal cells can exceed the rate of entropy production of cancer cells. Thus, it was concluded that reversing the flow of entropy in coexisting normal and tumor tissues can arrest tumor development due to reverse signal transduction in the tumor-host entity[26,27]. Despite these promising theoretical insights, practical implementation remains hindered by significant challenges. One major limitation is the current lack of adequate imaging modalities capable of visualizing dissipative structures in real-time. Such imaging techniques are essential for providing biofeedback during experimental interventions, allowing researchers to monitor changes at cellular and systemic levels, and adjust treatment protocols accordingly.

The interplay between an electrically charged tumor and its surrounding cellular environment can be understood through the lens of electromagnetism and dissipative structures. As a tumor exhibits unique electrical properties[28-31], it alters the state of nearby conductive mediums, including adjacent cells and intercellular fluids. This alteration manifests as a dynamic electrical impedance landscape that reflects the tumor's metabolic activity and heterogeneity. When external stimuli interact with this environment, they can induce modifications in the tumor's metabolism, further influencing its electric field. Consequently, the changes in electrical parameters not only signify the tumor's characteristics but also reshape the electrical landscape around it, creating a feedback loop where weak external effects can lead to significant alterations in both tumor behavior and its surrounding cellular milieu.

Imaging of dissipative structuring in cancer research is crucial for understanding the complex dynamics of tumor behavior and progression. This imaging can provide valuable insights into how cancer cells interact with their environment, adapt to therapeutic interventions, and develop resistance. Effective visualization is essential for translating these insights into targeted therapies, as it enables researchers to identify critical patterns and mechanisms that drive tumor evolution and response to treatment. The fact that tumors grow over months or years while cellular responses can occur within minutes underscores the need for a real-time approach to studying these processes. By employing techniques such as SEI, researchers can gain insights into how tumors communicate with their environment, particularly during critical moments when they respond to stimuli such as hypoxia or EMF. This approach allows for real-time assessment of intercellular communications and the structural changes that occur within both the tumor and its peritumoral environment.

Skin, the largest organ of the human body, serves as a critical interface between the internal physiological processes and external environmental factors. Its complexity and dynamic nature make it an intriguing subject not only for dermatologists but also for oncologists and physicists. The study of skin, particularly in relation to melanoma—a malignant form of skin cancer—offers insights that extend beyond traditional molecular biology. Unlike other aggressive tumors, melanoma has a visually distinguishable morphological border. This distinct feature provides unique opportunities to study the spatio-temporal dynamics of this ecosystem within a living organism. By examining this macro-region through the lens of dissipative structures theory, researchers can gain a deeper understanding of tumor behavior and functional boundaries of this battle.

Fig. 1. Photo of the experimental setup of SEI and examples of SEL in normal and neoplastic areas demonstrating emergence of antiphase structures around tumor invasive fronts in response to nonthermal mm-EMF [35].

The advent of skin electrodynamic introscopy (SEI) marked a significant leap in dynamic/functional skin imaging. For the first time globally, back in the late 80s, SEI provided adequate visualization of the skin electrical impedance landscape (SEL), first in statics and then in dynamics. The innovation was particularly crucial in identifying electrophysiological portrait of melanoma at the background of visibly normal tissue[32-35]. In a series of experiments, it was established that in response to weak and ultra-weak stimuli, on and beyond the boundaries of melanoma, i.e. on visually normal skin, the surrounding landscape changes dramatically by emergence of high-amplitude coherent dynamics as in-phase and anti-phase structures, and wave-like processes. Perhaps this discovery did not fit into the contemporary broad/reductionist trend in cancer research. Also, in the absence of similar technologies to verify the claimed phenomena, the authors' publications may not have attracted the attention of oncologists. On the other hand, it should be recognized that the authors themselves did not fully realize, and therefore did not reflect, the systemic rather than molecular nature of these phenomena.

SEL of healthy skin is distinguished by the relative smooth chaotic landscape with low-amplitude fluctuations (Fig. 1a), and its high resistance/imperturbability to the used subthreshold test stimuli mechanical, electrical, EMF, MF, hypoxia etc., which allows it to be defined as an equilibrium system. The term "chaotic nature" in the context of skin refers to the complex and dynamic interactions that occur within the skin at various levels, including cellular and molecular processes. "When a system is far from equilibrium, small islands of coherence in a sea of chaos can appear. These structures are fragile; they last for a while, and then disappear, making way for new ones[36]". In the case of a tumor such as melanoma, disruptions in the normal regulatory mechanisms of the skin can lead to a loss of coordination among different cell types, altered signaling pathways, increased sensitivity to external and internal factors. As all our experiments with melanoma (11) have shown, the electroimpedance boundaries significantly exceed the optical ones. Moreover, they can also differ significantly in intra- and intercellular parameters. This suggests that a comprehensive assessment of tumor boundaries must consider varying scales of tissue examination to accurately delineate the peritumoral area. The functional boundaries of a tumor for a given physiological parameter are understood as dynamic thresholds within which the tumor demonstrates measurable responses of this parameter, indicating its adaptability and potential vulnerability.

By mapping out the SEL response to short and weak stimuli across different regions of the skin dynamically, it becomes possible to visualize areas where significant deviations occur—indicative of the tumor inhomogeneity and functional spectral boundaries of real and potential malignancy.

Given the above theoretical paradigm and our experimental findings, we can substantiate the following hypotheses:

- Among the various heterogeneous tumor segments exhibiting fluctuating states between disorder and order in response to external stimuli, there are those that are most metabolically active (e.g. younger tissue). They can be more briefly designated as emitters of entropy or negentropy*;
-The initial electroimpedance portraits of melanoma reflect quasy-stationary approximate flow boundaries of these emitters flow within tissues influenced by both prolonged oncogenic processes (spanning months to years) and immediate metabolic activities;
- The minimum functional boundaries of the peritumoral area should be assessed based on its maximum impedance boundaries. The width of this dynamic zone can be determined in response to weak energy or information impact: the contour line of sharp weakening of SEL oscillations is a demarcation indicator between healthy and tumor-affected tissue;
- The shape of the field/flow from a large (non-point) tumor is defined as a superposition of its emitters;
- Mitochondria** can play a primary role in establishing DS that shape the SEL and define functional boundaries of the peritumor.

**The idea of defining tumor parts or boundaries as emitters of entropy or negentropy hinges on understanding how these regions respond to external impacts. If the impact leads to increased disorder within the tumor cells—then one could argue that these regions are emitting entropy. Conversely, if certain parts of the tumor respond adaptively by organizing cellular processes or enhancing survival mechanisms under stress, they might be viewed as emitters of negentropy*

*** Mitochondria are often referred to as the powerhouses of the cell because they generate ATP through oxidative phosphorylation, a process that directly relates to negentropy.*

Data from 4 early experiments (3 melanomas and papillomatous nevus) were used for detailed analysis due to their similarity in the striking predominance of the impedance boundaries of the tumor over the visible ones. To further illustrate the dissipative nature of the discovered phenomena, we also briefly present results from a recent experiment conducted on a plant tissue.

Methods

The methodology used was described in our previous publications[30,31] Here we present some additional considerations in connection with the above hypothesis about the discovered phenomena as DS manifestations.

Briefly, SEI in contrast to conventional/stationary EIS, is a novel dynamic imaging modality. This is ensured by such technical advantages as unprecedented combination of three mutually contradictory features: high spatial and temporal resolution (1mm, 4ms/pixel totally for all 4 spectral parameters) over a fairly large area). That is, in time-lapse imaging mode:

- the time resolution is 4 sec and 8 sec for a frame of 32x32 mm^2 and 32x64 mm^2, respectively;
-spectral impedance parameters $Z=|Z|e^{j\varphi}$: $|Z_k|$,φ_k, $|Z_M|$, φ_M, where j is the imaginary unit, $|Z_k|$,$|Z_M|$ (further without parentheses), and φ_k, φ_M represent the modulus and phase at 2 frequences: 2kHz and 1MHz, respectively. These parameters reflect, simplifying, the resistive (ionic) and capacitive (membrane resistance/integrity) parameters of the inter- and intracellular environment, respectively.

The following were used as short-term stimuli: ischemia, extremely low-energy mm-EMF with low-frequency modulation and weak MF with a change in polarity (in the interval between frames to eliminate interference) as an imitation of ultra-low-frequency MF. In EIS studies of melanoma, the ratios of the spectral impedance parameters are also used as local (point) diagnostic criteria[39], for example, k= Z_k/Z_M or $Z_{k,,n}$-$Z_{M,n}$ (where "n" means normalised values). In the context of spatial imaging and the lack of a generally accepted term, we would define it as the "Ionic balance" (IB): a 2D dimensionless morpho-functional parameter, the understanding of which seems especially important in its 2/3D use[34].

To assess functional boundaries of a tumor, both correlation and fluctuation field methods were used, since they provide complementary information. Correlations can identify regions where cellular activities are in sync or out of sync—indicating potential areas of collective behavior or vulnerability—while fluctuations reveal heterogeneity that could signify adaptive resistance mechanisms or localized variations in treatment response.

By combining both approaches, one can gain a more complete understanding of tumor dynamics under energetic or informational stress conditions such as ischemia or mm-EMF, ultimately providing insight into reprogramming strategies that target both coherent structures and fluctuating behavior within tumors.

It is important to understand that when analyzing fluctuation or correlation fields, we record averaged dynamics that reflect coherent fluctuations in ensembles of thousands of cells. Accordingly, when discussing various intra- and intercellular processes,

we refer to their average or collective characteristics, which represent the state of the intercellular communication n network, as opposed to the generally accepted terms used in single-cell biology.

Results

Analysis I. Melanoma with satellite[34] (MS).

Here we present the results of a more thorough analysis of experimental data on previously discovered but not fully understood phenomena of the SEL test-induced structuring. The previously described experiment[34] included monitoring the melanoma zone (Fig.2) in response to a short-term ischemia by clamping the femoral artery with a cuff: before (2.5 min), during (1.5 min) and in the process of reoxygenation (4.5 min). Time resolution - 8 sec.

Fig. 2. Photo of MS. 1 -contour of the pre-existing nevus; 2- the MS visual boundary; 3 – peritumoral area and its impedance boundary (4) as a benchmark or impedance boundary of the tumor; 5- satellite zone; 6- the supposed zone of inivisible satellite.

1.1. "From chaos to order and back"

The transition from initially chaotic state to more organized patterns and back, when the external impact stops, emphasizes the dynamic nature of biological systems and their ability to self-organize—a key principle in the theory of DS[36]. The "order from chaos" concept suggests that while ischemic conditions introduce chaos at the cellular level (disruption of normal function), they can also lead to emergent properties where certain groups of cells organize their responses effectively—forming coherent structures that enhance survival strategies or adaptive mechanisms. However, it is essential to recognize that this order does not imply uniformity; rather, it highlights how some degree of chaos (fluctuations) is necessary for adaptability and resilience within tumor microenvironments

Fig. 3 illustrates such transition at the fluctuations maps of all extra- and intracellular parameters: Z_k, Z_M, φ_k, φ_M.

The fluctuations maps (Fig.3) were calculated for the initial, ischemic and reoxygenation periods (of 15 frames, i.e. 2.5 min each). In the snapshots, most of the above mentioned areas of interest are better distinguished in the φ_M-landscape (a4). As for the fluctuations maps of the preliminary (b) and post-periodic (d) periods, it is necessary to note the lesser relief and blurriness of the impedance boundaries of the tumor. The ischemic stage (c) led to a sharp contrast in the fluctuation fields and *new phenomena should be emphasized.* Compared with (c), omitting some *details* as a first iteration, the fluctuation landscape of the tumor clearly contrasts with the background in the form of:

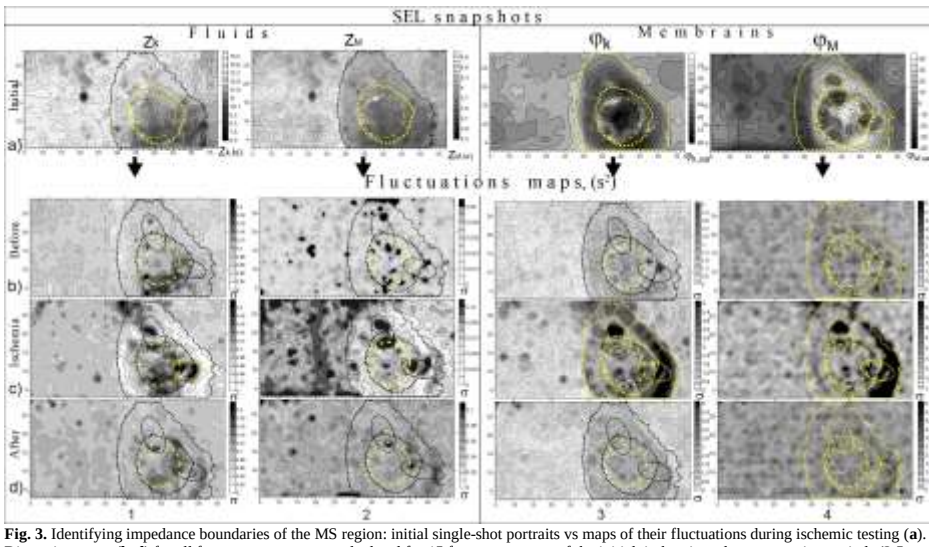

Fig. 3. Identifying impedance boundaries of the MS region: initial single-shot portraits vs maps of their fluctuations during ischemic testing (**a**). Dispersion maps (**b-d**) for all four parameters were calculated for 15 frame sequences of the initial, ischemic and reoxygenation periods (2.5 min each). The active area of the visible satellite and its supposed invisible "twin" are indicated by ellipses, $p<0.01$.
a) Among the snapshots, the most informative are the membrane parameters: the heterogeneous structure of the tumor area, including both elliptical areas, is especially clearly visible only in the φ_M-portrait (a4); In φ_k (a3), the MS zone appears entirely withn the boundaries of the impedance relief; the border of the pre-existing nevus can be discerned; **b)** In the initial dispersion fields, it is difficult to isolate the desired structures; **c)** The ischemic stage is manifested in the peritumor in the form of antagonistic oscillations c1,2 vs c3,4, with the exception of *elliptical zones, where activity has increased everywhere*.
Dispersion of normal tissues (except Z_M) remains almost unchanged, the large structure that appeared next to the MS on c2 is presumably associated with the reaction of the neighboring/feeding vessel (the walls of which became transparent at 1MHz frequency); **d)** Fluctuations falls to approximately the previous level (b).

- *Activity in the elliptical zones (both in liquids and membranes) stands out sharply, particularly marked in the intracellular level (c2);*
- *Weakening of the fluid impedance fluctuations approximately to zero* in peritumoral areas;*
- *Increase of the cell and intracellular membranes impedance fluctuations in peritumoral areas.*

* Similar effects were also registered in response to the weak MF exposure, Fig.S5.

In general, it is necessary to emphasize that all these dynamics occur within and beyond the impedance boundaries of the tumor "4" (Fig. 2), significantly exceeding the visible boundaries of the tumor "2" thus defining its functional boundaries.

1.2. Ischemia-induced dynamics around the tumor boundaries

- *Process of DS emergence;*
- *Antiphase structuring at boundaries;*
- *Reaction of 2D ion balance.*

The observation of autowave processes and antiphase structuring in biotissues serves as compelling evidence for their dissipative origins, demonstrating that biological systems can spontaneously organize into complex patterns when subjected to weak stimuli, consistent with the theoretical framework of DS. The phenomenon illustrates the dissipative nature of the melanoma zone through the interaction of various cellular ensembles in response to ischemia. The most

aggressive boundaries/zones of the tumor, like visible and hidden satellite, are often the most metabolically active and thus can be defined as main emitters of negentropia[36]. The activation of younger cellular ensembles in response to ischemia highlights a fundamental characteristic of dissipative systems: they maintain order and structure by exchanging energy/information and matter with their surroundings. This is evident as the hidden satellite zone, presumed to be more active, responds more vigorously to short ischemic events compared to its visible counterpart. As ischemia induces changes in the impedance landscape of cell membranes, coherent structures emerge on either side of the visible tumor border. The oppositely directed coherent structures signify a dynamic equilibrium that is characteristic of dissipative systems where energy dissipation leads to self-organization.

The initial* dynamics of the φ_k–landscape (Fig. 4a) is presented as the difference of the first two frames preceding the response appearance. However, the topology does not clearly reflect the configuration of tumor structures. It is only evident that the entire «3» zone (Fig. 2), stands out against the surrounding landscape due to the presence of antiphase clusters with noticeably increased amplitudes. It is worth to note the asymmetry of the peritumoral landscape, which obviously caused by the presence of a visible satellite and its invisible "twin" (indicated by ellipses). The areas "5, 6" start from inside the PN and go beyond the "2" border. The PN boundary clearly reveals itself here as antiphase structures on opposite sides of the border

Fig.4b demonstrates the first response detected at the 3[d] frame, i.e. after ab. 16 sec after clamping the blood circulation:

- appearance of a high-amplitude positively directed structure around the visible border with a maximum in the twin zone and a negatively directed structure in the satellite zone (the scale had to be increased by 2.5 times), with dimensions significantly exceeding the designated peritumoral border "4";
- distinct structuring of the second ellipse zone into oppositely directed dynamics of segments on both sides of the visual border “2” and its PN and thereby contrasting the boundary of the latter (enlargeв in Fig. 4f).

** The greatest response to ischemia is noted in Z_k, however, the choice of φ_k is due to its higher information content regarding the initial conditions, presumably associated with the influence of the measurement microcurrents.*

The next difference image/residual (c), compared to the previous one, reveals red structures completing the border “2” encirclement. It is especially marked on the side of the twin, with intriguing absorption of both nevi at a speed of about 1-2 mm/sec (marked smoothing of the entire landscape is explained by coarsening of the scale range). This transition was mainly complete by 1 min. Fig.4e presents the resulting change in the φ_k–landscape over this period. Its further modifications in the reoxygenation stage are presented as correlation fields in Fig.5 and as fluctuation maps in Fig.3c3.

Similar dynamics of response to ischemia can be traced on all 4 parameters of SEL. In general, this response also manifested as ionic balance $k = Z_k/Z_M$ (raw maps: Fig.3a1,a2). Fig. 4g represents its initial landscape, on which the contour k practically coincides with the impedance border of the tumor “4”. The response to ischemia manifested itself as the appearance of two red coherent structures by 5-10% exceeding the background (Fig. 4h) and noticeably expanding the borders 4. In this case, the increase in k is associated with a predominant increase in the extracellular impedance Z_k in response to ischemia. At the reoxygenation stage, these differences are leveled (Fig. 4i). However, distant k-profile abnormalities (Fig. 4i) may indicate visually indistinguishable metastases, as shown below (Fig. 6b).

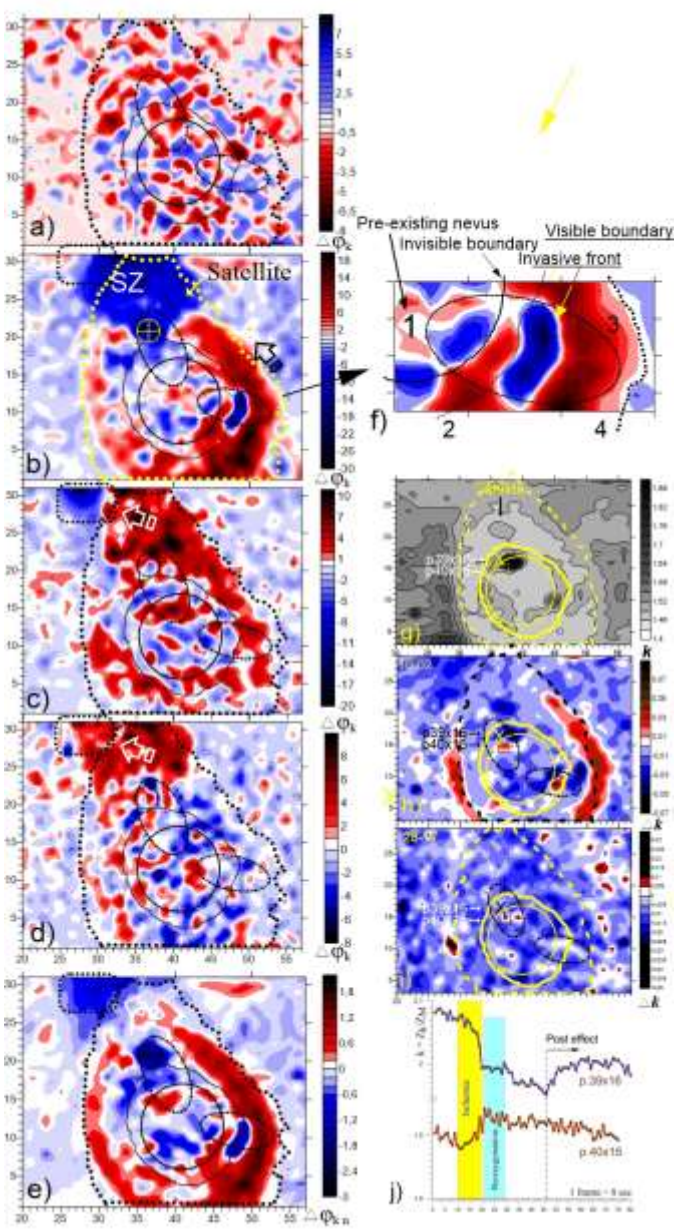

Fig. 4. Ischemia-induced wave in peritumor as cell depolarization/hyperpolarization (φ_k). The difference normalized maps of the first 4 frames (temporal resolution 8s) demonstrate weak but noticeable initial dynamics of the MS and its surroundings followed by high-amplitude clustering, $p<0.01$. a) Photo of the MS zone: 1 -contour of the pre-existing nevus; 2- the MS visual contour; 3 – peritumoral area and its impedance boundary (4) as a benchmark; 5- satellite zone; 6- the supposed zone of its not yet manifested “twin” satellite. b) (scale range expanded 3 times) Initial dynamics immediately before the ischemia effect in the form of a difference image between normalised 3d and 2d frames; c) similarly, 4th - 3rd. Further advance of the leading edge with absorption of the remnants of blue, beginning of fading of the trailing edge; d) 5th - 4th. Emergence of antiphase structures around the border of the pre-existing nevus shown by arrows (b); e) Normalized map of 8th -2d recording the completion of the transition process. $p<0.001$

g-i) maps of the original IB k and its changes during ischemia and oxygenation as difference images; **j)** time dynamics of k of pixels located on opposite sides of the PN boundary.

Note: All the main events inside the visual and impedance boundary occur in the zone of ellipses and in the direction specified by them. Moreover, the wave seemingly originates from the area of younger satellite. The absorption of the blue structure by the red one can be associated with cooperative effects of depolarization and subsequent hyperpolarization of cell membranes.

The phenomenon of antiphase dynamics of φ_k at the tumor boundaries, noted above, also manifests itself in the dynamics of ionic balance k, which is shown in the graph of two border points of the PN, Fig. 4j. It is noteworthy that in the "twin" zone, the points of antiphase response are located on the visible border of the tumor, at the epicenter of the wave's origin. The graphs also show that in the post-effect stage, differences in the course of the *k*- curves again appear. Moreover, this latent period approximately coincides with that which was revealed as a result of burning of plant tissue (Fig. 19).

Melanoma boundaries on the φ_k-correlation fields

- *Ordering and disordering phenomena in ischemia and reoxygenation*

Correlation fields of relative averages of the φ_k-landscape for each stage are shown in Fig. 5a-d. Main features:

(a) Before: Indistinct topology with minor differences of the tumor in the form of negative microclusters;

(b) Ischemia: Sharply antiphase negative clustering around visible and invisible boundaries ($-1.0 \le r \le 1.0$), expansion of the first beyond "4 (compare with Fig.4b), appearance of larger clusters in the distance;

(c) Reoxygenation: Reversal of negative structures, especially those surrounding the tumor - from $-1.0 \le r$ to $r \le 1.0$. Minor changes in the background (not counting the almost complete smoothing of negative clusters);

(d) Post-effect shows a clear opposite trend to the previous stage: a weakening of coherence within "4", especially in the wave generation zone, at the background of sharp increase in the coherence of the entire environment.

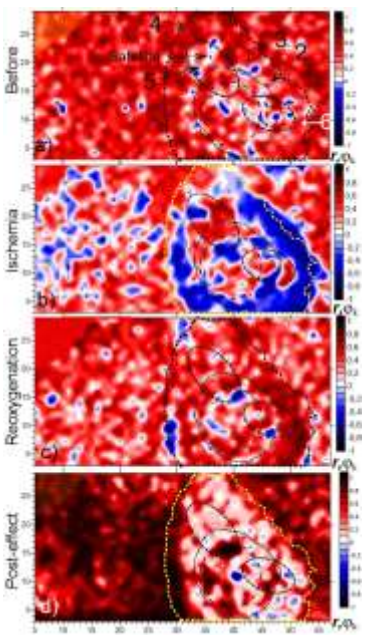

Fig. 5. Coherent dynamics of φ_k- landscape during the whole experiment. Correlation fields relative to averages reveal ($p<0.01$): **a)** Initial presence of several remote microclusters and a larger number/size in the "4" boundaries; **b**) sharp antiphase structuring of "3" ($-1.0 \le r \le 1.0$), with a basically important exit beyond "4"; **c**) Relatively rapid relaxation process with disappearance of most antiphase clusters;
d) Establishment of a maximum stabilization mode during the post-effect period with the disappearance of antiphase clusters everywhere except "4". Conversely, "3" stand out with even less variability than before.

<u>Analysis II</u>. Superficial Spreading Melanoma[33] (SSM)

In contrast to the upper, there were no visible satellites in this case, Fig, 6a. However, the zone of extended ion imbalance (within ~10% from the background $k= Z_k/Z_M$ values) was detected[33], Fig.6b. There were also other peculiarities:

- The most pronounced direction of this zone starts from PN "1" and, through the intermediate zone "5", ends with suspicious structure "4". The PN boundaries can be distinguished in the photo (Fig.6a), and also -what is especially interesting- in the mitochondrial φ-landscape, Fig. 6b;
- Contrasting boundaries of the mitochondrial landscape φ_M, which far exceed the visible size of the tumor, Fig. 7b: mitochondrial dynamics are known to be critical for the metastatic potential of cancer cells, as their movement to sites of high energy demand supports invasive behavior.

Another reason for choosing the SSM data for detailed analysis was assessment of both effects: energy (ischemia) and informational one (MF/EMF) used in this experiment. It was also significant that in both presented cases similar ischemic test protocol were used, i.e. stopping blood circulation in the limb with a cuff for 1.5 minutes.

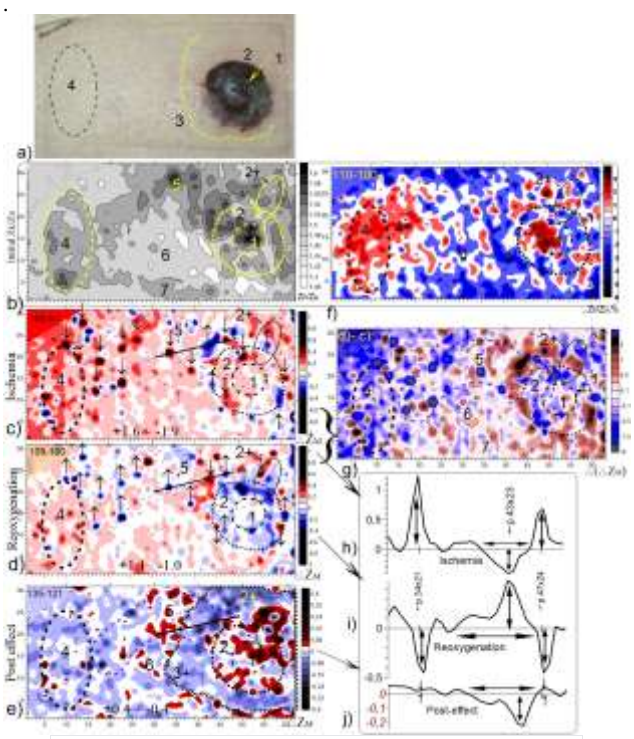

Fig. 6. Ischemic responses and localized tumor effects at cytosol impedance level Z_M. A photo of SSM. 1-PN, 2-visible boundary of SSM, 3- boundary of φ_M landscape (see Fig.7b), 4,5,7- zones of abnormal IB $k=Zk/Z_M$, 6-intermediate region; **b)** calculated map* of k; **c)** Difference of normalized Z_M images for the ischemia period (frames 100-91, i.e. ab.1.5min). Arrows ↓↑ indicate peak points with antiphase dynamics **d)** Similarly, the reverse changes of all marked peak points during reoxygenation (frames 109-100); **e)** Difference map for the post-reoxygenation period (frames135-121). Line 3+ denotes the advance of the front 3; **f)** map of k changes during ischemia; **g)** Difference map of (**d**) and (**c**); **h-j**) Profiles drawn through the peak points 34×21 and 47×24 (marked with a line at **c** and **d**), $p<0.001$.

2.1. Energy impact

2.1.1. Emergence of functional boundaries from the peritumor microclusters. Cytosol Level

- *Dynamic microclusters in the ion imbalance zone;*

- *Ischemia-induced expansion of boundary microclusters;*
- *Post-effect contrasting of functional abnormalities.*

The difference image of the Z_M landscape during ischemia (Fig. 6c) revealed in region “5” a family of peak points (microclusters) in phase with the background and a couple of intratumor points(«2» marked ↓. On the contrary, several out-boundary points marked ↑ showed antiphase dynamics.

The stage of reoxygenation reveals reversal dynamics with phenomenon of expansion of the area of these boundary clusters. forming thus a coherent structure around “2”, what is better seen in the profiles of Fig.6i,j. The difference between the two stages (Fig.6) shows the resulting formation of an antiphase structure at the tumor border.

The effect of simultaneous increase in the width and amplitude of the peak points is also shown in Fig. 6j using an example of dynamics of the profile drawn through points 34×21 and 47×24 marked by a thick line in (c) and (d).

The post-effect period is represented by the difference map Fig. 6e. It shows the systemic response manifests itself as a total reversal, but with distinct spatial differences, which can be also seen in corresponding relief in Fig. 6j:
- appearance of "3+" as a new functional boundary of coherent peritumor zone (blue);
- smoothing of the entire landscape, especially to the left of "3+", with the disappearance of point anomalies, which is clearly visible when comparing profiles p.34×21 with p.47×24, Fig. 6j;
- contrasting "1" and "2+" (red) due to a clearly smaller attenuation. In addition, similar/opposed behavior (red islands) should be noted outside "3+, especially in zone "5".

It should be especially emphasized that mitochondrial landscape φ_M also demonstrated a very extrodinary behavior in the particular area: the "3_3+" strip and the "6" area appeared twice (i.e. earlier than that of Z_M) -during the ischemia - on the fluctuation field (Fig. 7d), and during the post-effect - on the correlation field, Fig. S2.

Note. Basically similar process of formation antiphase structure at the melanoma boundary from initial microclusters in response to mm-EMF also applies to the case[35, Fig.15] shown in Fig. 1.

2.1.2. Ischemia-induced reorganization of the φ_M fluctuation and correlation fields

- *“Order from chaos”: emergence and advancement of φ_M boundaries;*
- *Systemic phenomena in the post-reoxygenaton stage.*

In the peritumoral zone of melanoma, in response to ischemia, a sharp increase in the level of spatial fluctuations of mitochondrial membranes φM (suggesting higher mitochondrial activity) was detected. This is particularly noticeable beyond the peritumoral border, and obviously means an expansion of this functional border. During the reoxygenation period, effects of both weakening of the fluctuation field fluctuations and its smoothing were also observed.

The initial snapshot of φ_M-landscape is presented in Fig. 7b. Its main features:
- The peritumoral mitochondrial boundary “3” stands out in contrast. Its configuration reflects the topology of the internal structures, which (similar to the case of MS, Fig.2), allows us to imagine “2” and “2+” as emitters of negentropy;
- Zone “4” stands out noticeably;
- The visible boundary “2” is mainly indistinguishable.

Fluctuation field of the preliminary stage (Fig. 7c), despite the zoomed-in scale, is a featureless chaotic landscape.

The ischemic stage (Fig. 7d) demonstrates emergence of a new ordered structure “3_3+” (σ >45) at about totally increased fluctuation landscape. A significant exception are two sections in “1” and “4”, where the ordering effect is visible with an unchanged average amplitude of pulsations characterizing their similarity, which is also shown in the relief of Fig. 7d’.

At the reoxygenation stage (Fig. 7e), one can see a significant and
ubiquitous weakening and smoothing of the fluctuation landscape compared to the original (c).

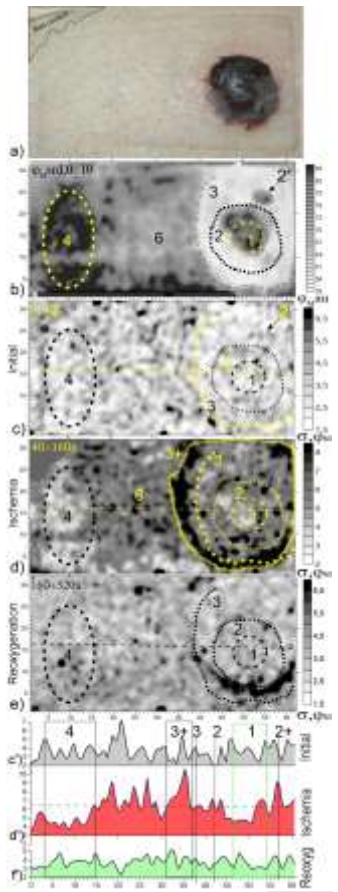

Fig. 7. Radial expansion of mitochondrial functional boundaries in the fluctuation field during ischemia. **a)** Photo; **b)** Initial φ_M-landscape; .**c)** Initial dispersion field (the scale has been increased); d) Increased fluctuations and expansion of the boundaries to “3+” in the response to ischemia; **e)** Weakening and smoothing of the fluctuation landscape; **f)** Landscape profiles (dotted lines in the middle of the c,d,e frames), p<0.01

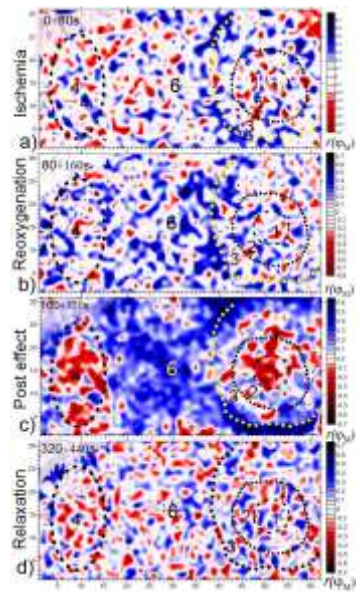

Fig. 8. Correlation fields of φ_M for all stages. It is seen that the maximum synchronization and the corresponding contrast of the φ_M landscape occur at the post-effect stage with subsequent rapid desynchronization.

This process of ordering/disordering of the φ_M landscape is also manifested in the correlation fields of Fig. 8. It is evident that the maximum synchronization and the corresponding contrast of the φ_M landscape occur at the post-effect stage with subsequent rapid desynchronization.

Note. Comparative analysis of similarities and differences in the spatial dynamics of other SEL parameters is beyond the scope of the predominantly demonstrative format of this article. Formation of the "3+" and structural movements in zone "6" is shown in Fig. S2. The global "step-by-step" and endpoint changes of φ_M landscape during the entire test are presented in Fig. S3.

2.2. Information impact: EMF/MF-induced reorganization of SEL

The assumption that EMF has a more specific effect on the tumor macroenvironment compared to ischemia is grounded in the idea that EMF/MF can modulate cellular communication and metabolic processes in ways that ischemic conditions cannot replicate.

The entire course of the experiment is shown in Fig. 9a, in which the mm-EMF/MF part is presented in 7 stages of 1 min each. (A 10-min break was made between the EMF/MF test and the ischemic one.)

To double the temporal resolution up to 4 s/frame, the SSM was read in 1 half of the scanning head ($32\times32mm^2$).

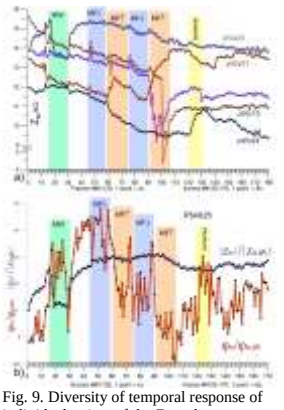

Fig. 9. Diversity of temporal response of individual points of the Z_k and φ_M landscape throughout the whole experiment. **a)** The Z_M time courses of five randomly selected pixels; **b)** A point* of the 2+ area demonstrates the high sensitivity of membrane impedance compared to liquid impedance (as relative to the averages), p<0.001. *In coordinates 64x32

2.2.1. Temporal dynamics of some pixels

- *Locally increased sensitivity of φ_M compared to Z_M*

Fig. 9a shows the time curves of five randomly selected pixels inside and outside the contour "2", thus demonstrating different scenarios, noticeable differences in response time, and large differences in the sensitivity of the cytosol impedance Z_M to each of the applied stimuli throughout the experiment. In principle, for each of these points, as for all the others, it is possible to conduct a correlation analysis to identify the coherence zone surrounding it. However, since such voluminous work is best left to AI, we had to limit ourselves by spatial fluctuations of Z_M and φ_M in response to mm-EMF and their average response to all four stages of MF.

Anomalies of the "2+" zone, in particular, manifested themselves in the initial dynamics of the pixel p. 54×25: the antiphase dynamics of Z_M (Fig.9a) and the high amplitude fluctuations of φ_M (Fig.9b). Many other points, especially at the mitochondrial level, with abnormal initial dynamics are seen in the fluctuation maps, Fig.11b,g.

Interestingly that Z_M in "2+" (p. 54×25) exhibits high sensitivity, unlike that of φ_M, to only one factor – mm-EMF, Fig.9a.

Note. In the context of the ischemic test results, it is worth emphasizing that the membrane response (φ_M) of some specific regions was also significantly more marked than that of the fluid resistance (Z_k,Z_M), which is especially noticeable, for example, in the intriguing "2+" zone, as shown in Fig. 9b.

2.3.2. Internal and external boundaries in the fluctuation field of φ_M

- *Manifestation of the PN stroma as an internal morphofunctional border;*
- *Expansion of external functional boundaries similar to that in the ischemic test.*

Fig. 10 presents fluctuation maps of φ_M for the four first stages of the EMF/MF experiment. (The entire set of φ_M fluctuation maps is shown in Fig. S4). Fig.10b depicts initial landscape, that is more chaotic than not;

Fig. 10c) shows that the impact of mm-EMF leads to a sharp ordering of the fluctuations landscape and manifestation of:

- associated structures in zone "1" (presumably stroma of the PN) and 2+;
- a girdle structure along line 3 – the initial quasi-"stationary" boundary of the mitochondrial landscape in real (non-fluctuating) parameters.

With the switching off of mm-EMF, the collapse of these structures begins (Fig.10d), but subsequent exposure to MF↓ (Fig.10e) restores the ordering with an even greater amplitude of fluctuations.

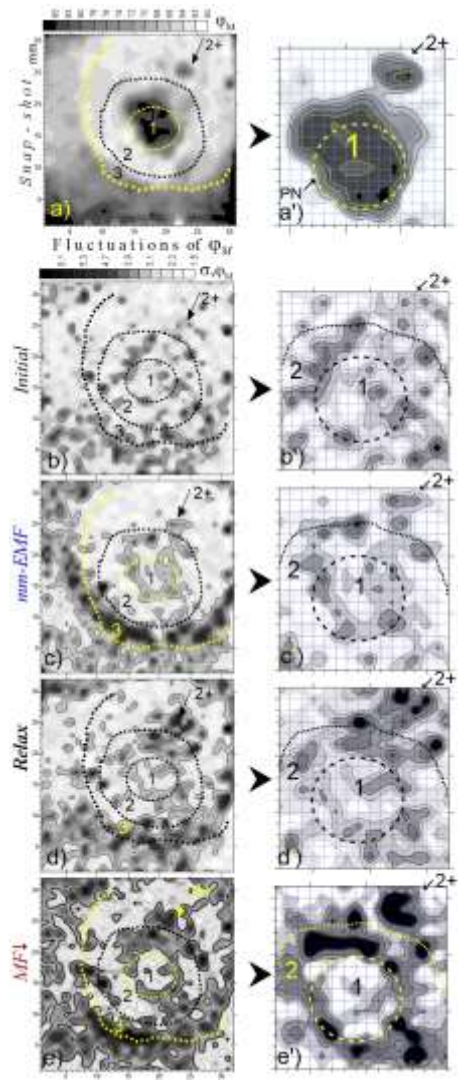

Fig. 10. The mm-EMF/MF$_\downarrow$-induced φ_M fluctuations. **Top row)** The φ_M and Z_M snap-shots; **b-e, g-j)** their fluctuation maps; **a'-e')** φ_M in an enlarged scale; p<0.001.

2.3.3. Ordering-disordering phenomena in the correlation fields of φ_M and Z_k

- *Emergence and reversal of the mitochondrial front in response to mm-EMF/MF;*
- *Dual ordering of Z_k -correlation field in response to EMF and MF, characterized by predominance of high positive correlation in the background, juxtaposed with isolated regions/clusters of negative correlation (supposed DS) at the peritumor area;*
- *Reverse migration of Z_k clusters to the tumor border.*

Fig. 11 shows differences in the processes of ordering the φ_M and Z_k landscapes throughout the entire EMF/MF experiment in the form of correlation fields.

The most significant features of the φ_M and Z_k dynamics are:

1) (a,e) Both landscapes reflect predominantly chaotic dynamics, where individual coincidences with the tumor structure are probably explained by the influence of measuring microcurrents[51].

In both cases, similarities were observed:

(a) large-scale structuring of φ_M field throughout the field and significantly increased clusterization in the PN "1" (see also the **a'** relief);

(e) small-scale structures Z_k, particularly noticeable in the "2+" zone and in the left upper peritumoral zone, i.e. in the same peritumoral area where they appeared in response to ischemia (Fig.5).

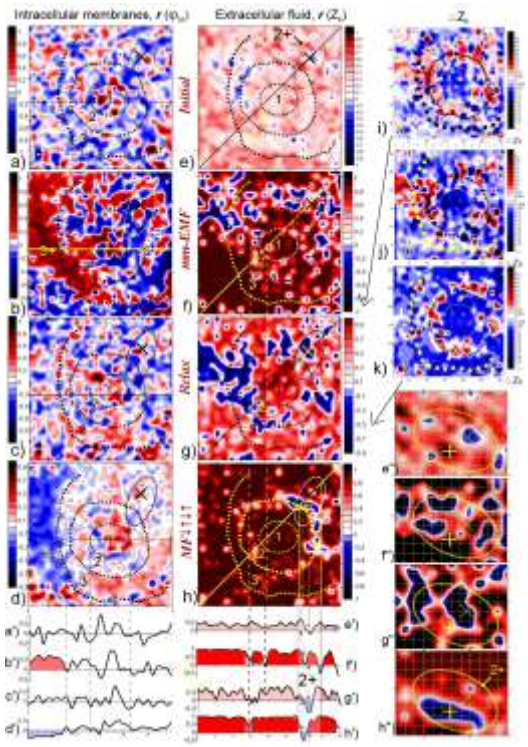

Fig. 11. Effects of clustering/declustering and DS movement. The φ_M and Z_k correlation fields relative to average: **a,e)** Initial stages**; b,f**) The mm-EMF stage; **c,g**) Relaxation stage: **d,h)** The MF exposures (see Fig.8). **Bottom**) Profiles of a...h .(solid lines) **Right column**) The DS effect of "reversible structuring": **i-k)** Difference Z_k maps during the relaxation period (**g**); **e''..h''**) Enlarged fragment of **e_h** showing antiphase dynamics of supposedly true boundary points marked as "×" and "+" in (h). p<0.01.

2) (**b,f**) Both landscapes reflect the process of sharp ordering in the response to mm-EMF. At the same time, in (b), as in the response to ischemia (Fig.6d), the *same phenomenon of emergence of the coherent "3_3+" structure of φ_M* is evident. The response of the Zk (f) changed towards greater polarization of the whole landscape thus highlighting areas with antiphase dynamics against the background of the majority with r≤+1.0. This impressive phenomenon of ordering is clearly visible in the profiles. (e'-h'). (Notably, the topology of negative clusters basically corresponds to that under hypoxia Fig. 6c).

3) (c,g) At the relaxation stage, one can see the reverse dynamics, i.e. disordering of the field φ_M and decrease in the coherence of the red background of Z_k (g') with amazing simultaneous growth of the blue structures, as a continuation/aftereffect of the response to mm-EMF. It should be borne in mind here that the correlation field was calculated based on 15 frames of each series and thus represents an averaged estimate of this dynamics. To reveal it in more details, difference images of the Z_k for this period were calculated. Fig. 11 i..k show that this process occurs in the form of *contraction of the family of dissipative structures* (blue) to the visible boundary "2". (Without detecting this dynamics, the following changes. i.e. in ***h,*** could be erroneously attributed to the action of the MF). In Fig.11k, the original feature of the "2+" zone as the end point of this "contraction" (and, hypothetically, a separate emitter of negentropy) appeared in the form of a separate DS marked with "×".

4) (**d,h**) During the MF stage, high ordering of Z_k (r ≤+1.0) manifested itself almost on the entire landscape "h". From the "blue" pattern basically only "2+" zone with a few neighbouring clusters at the tumor border remained.

To emphasize the antiphase nature of two adjacent points this zone, the figures (e''-h'') present the process of the "2+" rearrangements on a larger scale. These points ("×", "+") are probably located on opposite sides of the true morphological border of the tumor (in clarification of the approximately designated boundary "2").

Regarding the φ_M dynamics, the most significant is the secondary manifestation of the "3_3+" structure as a negative correlation. In addition, a noticeable smoothing of the landscape can be noted (d,d").

In general, the main similarity of the collective impedance dynamics of mitochondria and cell liquids in response to weak energy and information impact (ischemia, non-thermal EMF) is that in both cases there is an expansion of functional boundaries in the form of activation and propagation of the front dynamics of *corresponding* initial impedance landscape. A significant difference is that, unlike the mitochondrial response, the cellular fluid response is manifested predominantly only on the outer contour of the tumor, Fig. 15.

<u>Analysis III</u>. Impairment of EMF/MF-Induced Structuring Mechanisms in Irradiated Melanoma. *A sharp weakening or absence of most of the above phenomena, especially antiphase structuring of tumor boundaries and autowave processes.*

The protocol for this experiment with irradiated melanoma is similar to those described above: mm-EMF and a sequence of oppositely directed MF fields (Fig.9a).

Fig. 12a-d demonstrates a great similarity of the initial impedance landscapes: ionic balance k= Z_k/Z_M (b), cellular φ_k and intracellular (φ_M) membranes (c,d). Fig. S12e-g show the fluctuation landscapes of these parameters at the stage of the greatest response – to mm-EMF. The only response to mm-EMF was expressed at the level of the cell membranes in the form of the region of the greatest oscillations, Fig. S12f. Moreover, the dimensions of this response, as in the above cases, significantly exceed the initial impedance boundaries of the tumor. In contrast, the response of the ion balance and intracellular membranes is practically indistinguishable against the background noise.

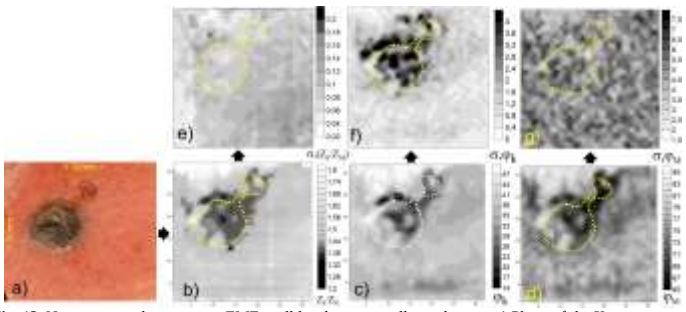

Fig. 12. No pronounced response to EMF at all levels except cell membranes. **a)** Photo of the X-ray irradiated melanoma; **b-d)** initial impedance landscapes: ionic balance k= Z_k/Z_M (**b**), cellular φ_k (**c**) and intracellular (φ_M) membranes (**d**); e-g) their corresponding fluctuation fields in the stage of greatest response (mm-EMF).

Fig. 13b shows the manifestation of the maximum response of φ_k in the form of difference images. It is worth noting the left - predominant - side of this response: at the tumor border of this region, an antiphase structure emerges in the next two stages (c,d), marked by arrows.

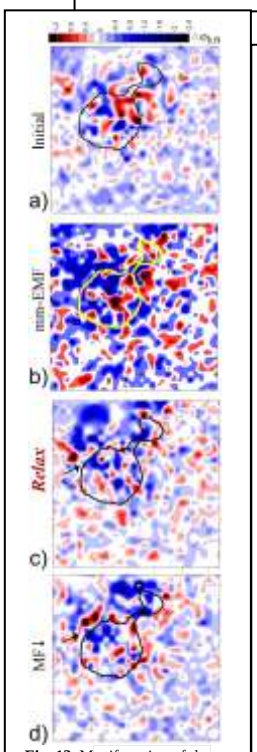

Fig. 13. Manifestation of the maximum response of φ_k (b) and subsequent emergence of anti-phase structure at the tumor boundary, marked by arrows (c,d). Normalised difference images of the first and last frames of each series.

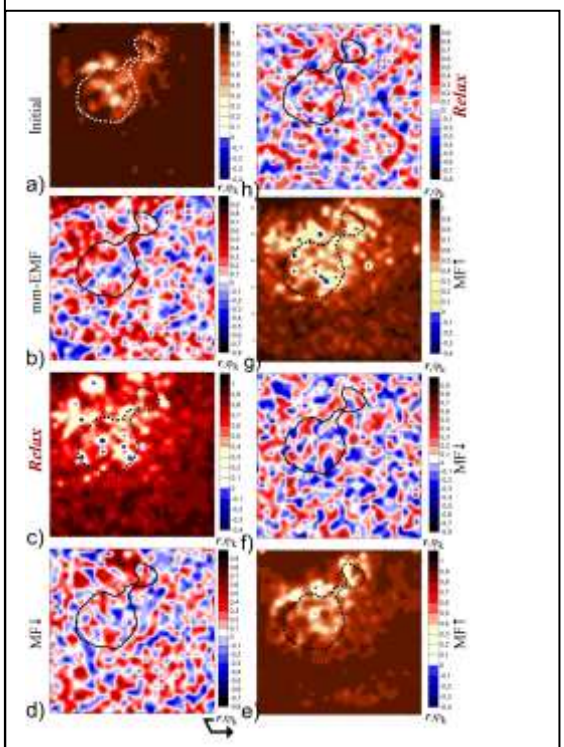

Fig. 14. Coherent dynamics of φ_k- landscape during the whole experiment: correlation break at the tumor area (a,c,e,g) and ordering phenomenon of the entire landscape (b,d,f), $p<0.01$.
Note: For maps a,c,e,g and b,d,f, the color scales were selected strictly the same for each of the groups.

Figures 14a_h depict correlation fields of the φ_k-landscape throughout the experiment, thus demonstrating:
- 4 cyclic discrete transitions between two dynamical regimes of spatial correlation in the rhythm of the applied stimuli;
- inexpressive contrast of the tumor zone in the mm-EMF stage (b);
- initially relatively weak manifestation of the tumor as a coherence anomaly (both in size and magnitude) with its subsequent 3-fold manifestation as a correlation break - with expansion of the anomaly zone and the appearance of point areas of anticorrelation ($r \leq 0.4$).

In our opinion, there are sufficient grounds to assert that the boundaries of this abnormal zone correspond to the functional boundaries of the tumor at the level of cell membranes.

The very absence the above phenomena of antiphase structuring and autowave dynamics at the level of inter/intra-cellular media in the context of radiation-induced damage to intercellular communications serves as practical evidence supporting the hypothesis regarding their dissipative nature.

Discussion

Previously[32-35], it was shown for the first time that the impedance boundaries of melanoma significantly exceed its optical dimensions and it is this "impedance peritumor" that reacts sharply to soft stimuli such as short-term ischemia and non-thermal electromagnetic fields. The analysis confirmed previous findings and a whole range of new biologically significant phenomena new effects have been identified. We suggest that these phenomena provide substantial evidence supporting the hypothesis proposed here regarding the effects of self-organization and dissipative structuring at the tissue and cellular levels. From the point of view of the DS theory, the revealed impedance boundaries of the tumor can be interpreted as an effective zone of entropy/negentropy flow from the tumor, and, respectively, the functional boundaries of the tumor can be assessed by the advancement of the impedance front caused by stimulation of the entropy flow, Fig. 14.

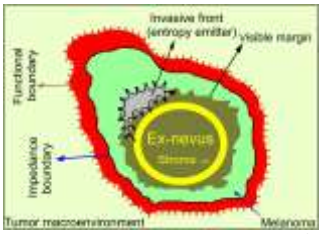

Fig. 15. Schematic representation of melanoma and its boundaries. Configuration of the functional boundary is determined by the topology and aggressiveness of the

The abundance of the listed phenomena is explained by the "discoverer effect" of a previously unknown object – the electrical impedance landscape of the skin, and its spatial and temporal dynamics. However, despite the promising nature of these findings, we acknowledge that the limited sample size and inherent heterogeneity among the studied objects pose challenges for comprehensive biological interpretation. The variability in tumor characteristics may lead to difficulties in drawing generalized conclusions from our observations. Nevertheless, we propose that most of these phenomena can be contextualized within the "Order from chaos" concept of DS theory. It is also appropriate to recall that, in contrast to the electrodynamics of individual cells, the phenomena presented reflect the average collective electrodynamics of multi-thousand cell ensembles underlying self-organization processes. The results of Analysis I and II have been grouped according to the commonality of various manifestations of DS:

Local phenomena, "From chaos to order and back", i.e.:

- Abrupt shift in magnitude and depth of the impedance front in response to a weak stimulus or its cessation, Figures 3,4,5,6,7,10,11,13,14,16;
- Functional portrait of melanoma zone in fluctuations fields of intra- and extracellular SEL, Fig.3;
- **F**ormation of supposed DS around melanoma as a wave of cellular depolarization, Fig.4;
- Emergence of antiphase structures as markers of the tumor invasive front**,** (which determine the configuration of the functional border of the tumor) Fig. 4**;**
- Functional profile of the melanoma zone as an area of ionic imbalance, Fig. 4;
- Formation of antiphase structures from initial microclusters at the tumor boundary, Fig.6;
- Manifestation of stroma of pre-existing nevus, Fig.10;
- Smoothing of the fluctuations field, Figures 3,6,7,11
- Dual ordering of the Z_k correlation field in response to EMF and MF, characterized by predominance of high positive correlation in the background, juxtaposed with isolated regions/clusters of negative correlation (supposed DS) at the peritumor area, Fig. 11;
- Reverse migration of the supposed DS towards the supposed negentropy emitters, Fig. 11;
- Similarity between manifestations of information (EMF) and weak energy (ischemia) influence, Fig.15.

Systemic/post-effect phenomena:

- Emergence of the tumor resistance zone against the background (cell membrane level), Fig. 5c;
- Expansion of the peritumoral response front (cytosol level), Fig.6e;
- Antiphase correlation patterning (mitochondrial level), Fig.8c;
- Cyclic discrete transitions between two dynamical regimes of spatial correlation at the level of cell membranes in the rhythm of the applied stimuli, Fig. 14.

A number of similar effects and phenomena of self-organization and dissipative structuring have been registered not only in the area of such a malignant tumor as melanoma, but also in outwardly similar skin anomalies, such as a suspicious nevus (Fig. 1). These main common and complimentary features are presented in the Supplement Materials:

- ✓ Test-induced antiphase dynamics of impedance at the lesion's morphological boundaries, Figs. S12-S14;
- ✓ Expansion and propagation of initial impedance boundaries in response to EMF and ischemia, Fig.S13;
- ✓ Phenomenon of dual ordering of the correlation field in response to EMF and ischemia, Fig.S13;
- ✓ Emergence, propagation and relaxation of the complex of coherent in-phase and out-of-phase structures at the level of cell membranes during the breath holding, Fig.S14;
- ✓ Restructuring of the ionic balance landscape during the breath-hold period, Fig.S15.

The hypothesis about the dissipative nature of the revealed effects and phenomena is also confirmed by the results of our recent experiments with yeast and plant leaves. For example, Analysis IV (Supplement Materials) demonstrates: phenomenon of antiphase structuring of the impedance landscape of a plant leaf in response to a strong impact, as well as the subsequent post-stress effect, Fig.S16.

The "order from chaos" concept is particularly relevant in tumor biology, where chaotic cellular environments can lead to the formation and progression of tumors. The tumor microenvironment may initially appear chaotic, manifesting as irregular cellular arrangements, heterogeneous cell populations, and varying extracellular matrix compositions and signaling pathways. The impedance fluctuation fields reflect the dynamic electrical properties of tissues that can change in response to different physiological states or stimuli. In this context, DS are systems that maintain their organization through the continuous exchange of energy, information, and matter with their surroundings, leading to complex behaviors observed in SEL dynamics. This process is particularly relevant when considering the melanoma zone characterized by impedance fluctuation fields, where initial chaos may precede the emergence of structured tumor formations.

In the absence of external influences, and due to the relatively stable genetic and phenotypic traits, a tumor may be defined as a quasi-stationary structure exhibiting characteristics akin to a static entity over extended periods (months to years). However, *it is crucial to note that DS can only be identified in dynamic states. Without external stimuli or exposure to perturbations, these structures remain undetectable as they do not exhibit significant changes in their static form*. Moreover, in the absence of external

stimuli or disturbances, these structures may be obscured by background metabolic activity. Upon the application of external influences—such as measurement microcurrents—the tumor's behavior may shift from a quasi-stationary state to a more dynamic one. The more specific stimuli - ischemia or EMF - serve as triggers that reveal underlying structural organization within a chaotic landscape. These stimuli may induce changes in cellular behavior and tissue architecture, allowing for the identification of tumor segments that exhibit heightened sensitivity (Figs. 9,12) or are approaching a bifurcation state, which is crucial for identifying functional boundaries and understanding tumor dynamics. (This phenomenon parallels how sick or weakened organisms respond more acutely to environmental factors due to compromised systems.) The application of external stimuli not only reveals but also contrasts various tumor segments based on their sensitivity to these influences. Tumor cells at morpho-functional boundaries, particularly at invasive fronts, are often more responsive to environmental changes due to their dynamic nature and adaptive capabilities. These boundaries represent critical zones where cancer cells transition from benign growth patterns to invasive behaviors, making them prime candidates for observation under weak stimulus conditions.

In the short time frames of the experiments, the influence of the current metabolism on the impedance boundaries of the tumor "4" is relatively insignificant and therefore they can be considered as the boundaries of the effective zone of the current entropy/negentropy flow and - in the first approximation - as the minimal functional boundaries of the tumor. The presented images (Fig. 4,5,6,7,10,11,13,14,16) indicate that all test-induced dynamics occur within the impedance boundaries of the tumor, significantly exceeding its visible boundaries. The weak stimuli used can lead to a noticeable expansion of these boundaries, and at different levels of cellular organization this expansion can differ significantly (Figs. 4,5,7,10,11).

The observation of autowave processes and antiphase structuring around the tumor boundaries (Fig. 4) serves as compelling evidence for their dissipative origins, demonstrating that biological systems can spontaneously organize into complex patterns when subjected to weak stimuli. From the point of view of cellular biology, this effect can be explained by the tumor acidic microenvironment (Warburg effect) which is known to influence various cellular processes, including cell signaling, proliferation, and apoptosis. Cancer cells possess distinct bioelectrical properties characterized by a more depolarized membrane potential compared to their healthy counterparts[81]. The depolarization and hyperpolarization events occurring in cell membranes indicate a complex interplay between tumor cells and their microenvironment, which may lead to modifications in ion channel activity and signaling pathways within both intracellular and extracellular environments. This was also registered as a transit distortion of the ion balance not only around the visible border of the tumor, but also inside it (i.e. PN), Fig. 4h.

From the point of view of the theory of DS, following a brief ischemic event, a negentropy flow is initiated in the most aggressive region of the tumor. This flow induces a wave of ordering characterized by synchronized changes in the electrical impedance of cell membranes within the peritumor zone. Such synchronization reflects an emergent property typical of DS, where local order arises from energy/information dissipation, allowing for enhanced cellular communication and coordination. The propagation speed of this wave may depend on several factors, including the intrinsic properties of the cell membranes (such as ion channel dynamics), intercellular connectivity, and the biochemical environment that influences signal transduction pathways.

The case shown in Fig. 6 demonstrates the existence of another mechanism for the emergence of an antiphase structure at the tumor border in the form of an expansion of the area of the original microclusters in response to ischemia. (Basically similar dynamics was observed in reponse to mm-EMF in another case[35, Fig.15] shown in Fig. 1).

The k-landscape configuration and its dynamics (Fig. 6) are presumably related to the metabolic plasticity of melanoma cells and their crosstalk with the surroundings. It alters ionic balance through lactic acid production, affecting ion transport, and is closely tied to mitochondrial dysfunctions impacting bioenergetics[76]. Thus, it may indicate spatial directions for oncogenesis through ionic imbalance area "5".

In tumors like melanoma, cells often form microclusters or aggregates, enhancing survival under adverse conditions such as ischemia. These clusters can exhibit heterogeneous metabolic profiles, allowing some cells to survive even when others do not. Evidence supports that acidic regions surrounding melanoma are localized or clustered rather than randomly distributed throughout the tumor microenvironment. The presence of these clusters can affect the ionic balance in surrounding tissues due to altered secretion profiles (e.g., release of lactate, protons) and changes in membrane permeability. The post-ischemia expansion of clusters at the cytosol level shown in Fig. 6 further emphasizes the adaptive nature of cancer cells following stress events. Such expansions could lead to enhanced metabolic activity or altered signaling pathways that support tumor growth.

Magnetic resonance spectroscopy (MRS) visualized pH and exosome variations within tumors, revealing distinct clusters of acidity associated with aggressive tumor phenotypes[77]. Additionally, histological analyses have shown that these acidic zones often coincide with areas exhibiting high cellular density or necrosis, suggesting a relationship between metabolic activity and spatial organization within tumors[78]. These morphofunctional differences between the acidic regions surrounding the melanoma (Fig. 6c and Fig. 14b) and those further from the tumor edge may lead to contrasting reactions, such as the multidirectional response to hypoxia and an expansion of this zone in the impedance landscape in response to reoxygenation, which could potentially be used to identify them.

Understanding the localized nature of acidic areas surrounding melanoma and their sensitivity to short-term hypoxia has significant implications for treatment strategies. Targeting these specific microenvironments could enhance therapeutic efficacy by disrupting the adaptive mechanisms employed by cancer cells under stress conditions.

The initially expressed features of the quasi-static mitochondrial landscape (Fig. 7b) also manifested in its fluctuation fields (Fig. 7) in response to ischemia, as phenomena of advancing functional boundaries and increasing, then subsequently smoothing, the level of fluctuations. The sharp increase in mitochondrial impedance fluctuations during short ischemia reflects adaptive responses at both cellular and systemic levels within the peritumoral zone. From a cell biology standpoint, these changes can be related to local effects of mitochondrial fusion and fission under stress. In the DS context, the peritumor zone is characterized by

increased fluctuations where energy is utilized for cellular communication and adaptation—characteristics of a system striving for stability amidst chaos. The circular configuration of mitochondrial impedance boundary “3” (Fig.7b) may be related to their tendency to migrate to areas of greatest energy demand. This area is typically more responsive to environmental changes due to its proximity to healthy tissue, which may still receive some blood supply. Also, neoplastic mitochondria may exhibit heightened sensitivity due to existing dysfunctions caused by mutations or altered signaling pathways associated with cancer metabolism. The propagation of fluctuation fronts signifies an important aspect of intercellular communication that may influence tumor behavior and recovery mechanisms following ischemic events. Enhanced mitochondrial fluctuations may facilitate communication between tumor cells and their microenvironment, potentially influencing tumor growth and metastasis. Conversely, the smoothing effect within the tumor core “1”and zone “4” indicates that tumor cells may have reached a threshold where further adaptation is limited due to extreme hypoxic conditions or metabolic shutdown. Despite no change in amplitude, this smoothing can imply metabolic suppression and loss of heterogeneity. (It would be very interesting to confirm this, only now discovered, functional similarity between "1" and "4" using appropriate laboratory methods.)

The process of ordering/disordering of the φ_M landscape is also manifested in the correlation fields of Fig. 8. It is evident that the maximum synchronization and the corresponding contrast of the φ_M landscape occur at the post-reoxygenation stage with subsequent rapid desynchronization. The significance lies in understanding how tumors adapt to microenvironmental stresses, such as hypoxia.

We were particularly impressed by how purely informational influences, such as non-thermal mm-EMF and weak MF, elicited profound changes in the impedance landscape. These responses challenge traditional views on electromagnetic interactions and underscore a novel understanding of information transfer in biological systems.

Against the background of the mitochondrial landscape (Fig. 7b), the "2+" zone stands out for its similarity to the melanoma nucleus "1". The end-to-end graphical (Fig. 9) and subsequent fluctuation analysis (Fig. 10) revealed that this similarity is due to the high sensitivity of these areas to most of the effects used. In response to mm-EMF, this similarity manifested itself even more contrastingly in the φ_M fluctuation fields (Fig. 10) - in the form of two related structures: the PN stroma and the “daughter” structure "2+". These areas can exhibit a heightened response due to the presence of reactive stromal cells and altered extracellular matrix components that influence ion channel activity and cellular excitability[79]. Moreover, the identified phenomena may be associated specifically with mitochondria as mobile, dynamic, energy-transforming organelles that transmit signals to all cellular compartments and the entire organism[80]. *This may have profound implications for understanding tumor biology and treatment approaches. The enhanced spatial dynamics suggest that these regions may serve as critical zones for therapeutic interventions, potentially allowing targeted approaches that exploit their unique electrophysiological properties. Furthermore, the ability of these regions to rapidly turn on and off in response to EMF suggests dynamic adaptability that may influence tumor behavior, growth patterns, and responses to therapy. In terms of DS theory, the results imply that peritumor boundaries are not simply passive but actively engage in information exchange with external stimuli such as EMF. In our context, the enhanced spatial dynamics associated with EMF exposure may reflect a basic process of self-organization in these sensitive regions, leading to emergent properties that may influence cellular communication, metabolic processes, and overall tumor dynamics*.

Another striking manifestation of mitochondria as the DS phenomena is the existence of initial φ_M fluctuations (Fig.9b): according to the DS basics[36,54], initial irregular oscillations that evolve into substantial and stable alterations in a system’s behavior due to minor disturbances are indicative of the system’s dissipative characteristics. This phenomenon highlights how small influences can lead to significant changes in dynamic systems (Fig.10). In the context of post-ischemic conditions, the cellular and mitochondrial responses within the stroma of a PN can be understood through several biological principles. Ischemia affects cellular metabolism and mitochondrial function. The observed gradual weakening of the nevus core’s landscape may reflect alterations in mitochondrial impedance, indicative of changes in bioenergetics and cellular homeostasis. Mitochondria play a crucial role in energy production and are sensitive to environmental changes; thus, their impaired function can lead to differential relaxation rates between internal (neoplastic) and stromal mitochondria. This disparity could suggest that the neoplastic cells are undergoing stress responses due to ischemic conditions, while stromal cells might be responding differently based on their functional roles within the tissue microenvironment.

From the perspective of cell biology and DS theory, these observations can be interpreted as manifestations of complex adaptive systems where biological entities maintain order through energy dissipation. In this case, the post-ischemic response may represent a shift towards a new equilibrium state for both neoplastic and stromal cells as they adapt to altered metabolic demands and oxygen availability. The differences in mitochondrial behavior could indicate varying capacities for adaptation among cell types within the tumor microenvironment, which is critical for understanding tumor resilience and potential therapeutic targets.

In response to the mm-EMF/MF switching on and off (Fig. 11), two different scenarios of the correlation fields restructuring emerged at the mitochondrial and cellular levels. Interpreting these scenarios solely through the lens of cell biology is difficult; however, they can be conceptualized as examples of “order from chaos”:

- Emergence and reversal of the mitochondrial front as local coherent - positive and negative - spatial correlations. This demonstrates establishment of localized order amidst global disorder;
- Dual ordering of the correlation field in response to EMF and MF, characterized by a predominance of high positive correlation in the background, juxtaposed with isolated regions/clusters of negative correlation at the peritumor area, Fig.11e-h.
- Switching off EMF revealed the opposite effects - a decrease in the background coherence (Fig.11g) and the *phenomenon of reverse migration of the negative clusters to the tumor border* (Fig.11i-k);

- The following MF exposure resulted in return of the high correlation of the background plus an additional peritumor zone that was “freed up” by the displacement of negative clusters.

From the perspective of the DS theory, the chaotic fluctuations in the peritumor zone give rise to islands of negative polarity, while the melanoma zone exhibits a transition towards higher positive correlation. This phenomenon exemplifies “order from chaos,” as localized interactions and energy/information exchanges within the system lead to emergent patterns and structures that enhance biological organization amidst an otherwise disordered environment. Each scenario reflects different aspects of how dissipative structuring operate under varying conditions of order and chaos while suggesting mechanisms through which negentropy flows might manifest differently depending on structural organization at multiple biological levels. The emergence of high positive correlation in one region indicates a robust ordering process, likely driven by external energy inputs or internal feedback mechanisms that stabilize certain configurations. Conversely, the presence of islands of negative polarity in the peritumor area suggests localized disruptions or *competing dynamics within the overall system*. These negative correlations may arise due to factors such as resource depletion, competitive interactions among cellular populations, or differential responses to environmental stimuli. This duality reflects the non-linear nature of dissipative structures where regions can coexist with varying degrees of order and disorder. In summary, the interplay between ordered and disordered states in this context illustrates how complex systems can evolve dynamically under specific conditions, leading to heterogeneous patterns that are characteristic of dissipative structures.

There are analogs in biological systems where similar dynamics occur, e.g., (i) in neural tissues, individual neurons exhibit fluctuating electrical activities while simultaneously contributing to coherent patterns across networks; (ii) cardiac myocytes demonstrate synchronized contractions driven by localized electrical impulses but also maintain overall coherence necessary for effective heart function. These examples illustrate how both fluctuation-based dynamics (like those seen in mitochondrial ensembles) and coherence-based dynamics (as observed in intercellular communications) coexist in complex biological systems. In the context of the DS approach, while intercellular contents contribute to negentropy flow, their mechanisms differ from those of mitochondrial ensembles due to their reliance on extracellular interactions rather than intrinsic metabolic processes.

Comparing the φ_M and Z_k patterns (Fig.11) suggests that although spatial electrophysiological responses are expressed differently—mitochondrial responses are more pronounced in fluctuation fields due to their localized nature, while intercellular content responses are more pronounced in coherence fields due to collective behavior among cells—the underlying principles governing these processes remain interconnected through their contribution to overall cellular organization.

The emergence of structures around the tumor and within the stroma under EMF exposure indicates a form of DS, where non-equilibrium conditions lead to self-organization and increased spatial fluctuations in impedance. This phenomenon suggests that mitochondria can adaptively respond to environmental stimuli by reorganizing their functional architecture, thereby enhancing their capacity for energy production and cellular communication. Moreover, the transient nature of these structures upon cessation of EMF exposure implies a dynamic equilibrium between stability and fluctuation inherent in biological systems. The ability of these structures to reappear with renewed EMF exposure while maintaining their shape signifies an underlying resilience characteristic of dissipative systems. In contrast, the cytosol’s rapid but singular response may reflect its role as a more immediate mediator of cellular processes without the complex feedback loops present in mitochondrial function. This disparity underscores the importance of mitochondrial dynamics in understanding how cells interact with external stimuli and adapt over time.

The analogy between ischemia (an energy-related effect) and mm-EMF (an information-related effect) lies in their respective impacts on mitochondrial function. While ischemia primarily disrupts energy supply and induces stress responses, the mm-EMF exposure appears to modulate cellular communication and information processing within mitochondria. Both stimuli ultimately affect mitochondrial dynamics but do so through different mechanisms—ischemia through energy depletion and mm-EMF through informational modulation—highlighting the intricate interplay between bioenergetics and cellular signaling.

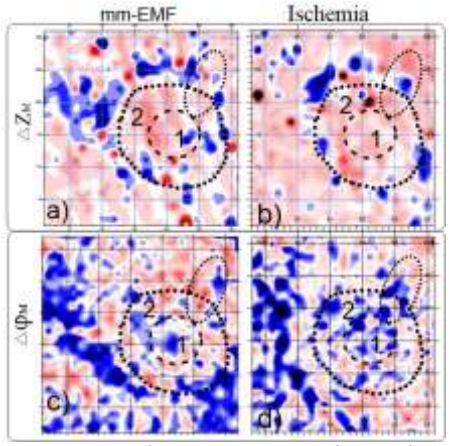

Fig. 15. An example of the similarity between manifestations of weak information (EMF) and energy (ischemia) influence:
a,b) Only on the outer contour of the tumor (cytosol level); **c,d)** On the outer and inner contour (mitochondrial level). Difference images of Z_M (up) and φ_M for the corresponding stages.

Both phenomena can be generalized under the concept of ‘order out of chaos’. They illustrate how biological systems maintain homeostasis or adaptively reorganize when subjected to stressors such as ischemia or non-thermal EMF. This suggests that both stressors elicit comparable biological responses across different cellular environments. Understanding these responses could have significant implications for developing treatment strategies targeting how tumors react to various forms of stress.

The phenomenon of reverse migration of the negative *clusters* (Fig. 11i-k) could be explained through cell biology’s insights on cellular response mechanisms combined with the principle that DS can undergo phase transitions based on external conditions[36,48,52,53]. When an external influence is applied, it may drive the system into a new state (e.g., tumor growth), but once that influence is removed, the system may revert back to its original state or another stable configuration. The reversible dynamics observed across various natural phenomena illustrate fundamental principles governing both living organisms and physical systems:

- *Cells exposed to growth factors proliferate; upon removal of these factors, they may cease division).*
- *Neurons exhibit synchronized firing patterns under certain stimuli but return to baseline activity when those stimuli are removed).*
- *Under nutrient-rich conditions, individual amoebae aggregate into multicellular structures that exhibit coordinated movement and function—a dissipative structure formed through collective behavior. When nutrients are depleted (removal of external influence), these structures disband back into individual cells).*
- *Ecosystems, like e.g. coral reefs, often display dissipative characteristics where species interactions create stable communities Changes in environmental factors can lead to shifts in community structure that may revert if conditions stabilize again.*
- *The Belousov-Zhabotinsky reaction showcases how chemical systems can form spatially organized patterns (DSes) under certain conditions but revert back to homogeneity when reactants are depleted or conditions change).*

The weak ordering effects revealed in the X-ray irradiated melanoma (Fig.12-14) seem linked to polarization and depolarization at membrane interfaces, which may play a crucial role in maintaining some level of coherence despite the overall disruption caused by radiation. Radiation therapy appears to stabilize the fluctuation fields of impedance within cellular fluids and mitochondria, suggesting a modulation of cellular bioenergetics. Despite this stabilization, cellular membranes maintain their integrity, as evidenced by their continued responsiveness to mm-EMF and MF. This indicates that while radiation therapy induces significant changes at the cellular level, it does not compromise the fundamental properties of cell membranes, allowing for ongoing interactions with external electromagnetic influences. Cell membranes might show less change relative to others since they serve primarily a protective role but still experience indirect effects through oxidative stress from free radicals generated during radiolysis. While polarization/depolarization alone may not be sufficient for coherence without proper coupling mechanisms (like gap junctions), it can contribute significantly when combined with other factors[82,83].

The tumor microenvironment can be conceptualized as a system of coupled oscillators where cancer cells interact with surrounding stromal cells, immune cells, and extracellular matrix components. This model helps explain reciprocal interactions between tumors and their environments. In the melanoma impedance landscape, the initial fluctuation field represents a state where there are varying levels of electrical impedance across different regions of the tumor. The presence of the tumor as a cluster with maximum fluctuations indicates areas of heightened activity or instability within its environment. This cluster's characteristics are crucial for understanding how it interacts with external influences.

When exposed to weak influences such as non-thermal EMF and MF, the dynamics of the entire correlation landscape undergoes a transformation towards uniform coherence. This shift implies that even minor perturbations can lead to widespread changes in system behavior, aligning with principles of self-organization where small inputs can yield large-scale effects.

In living organisms, similar discrete transitions can be observed:

-Neural Synchronization (In neural networks within the brain, neurons often transition between chaotic firing patterns and synchronized bursts depending on external stimuli or internal states).

-Population Dynamics (In ecology, species populations may undergo sudden shifts (catastrophic shifts) due to environmental changes—akin to bifurcations seen in physical systems).

-Circadian Rhythms (Organisms often display discrete shifts between different activity levels based on light exposure or other environmental cues).

Regarding tumor entropy emitters—hypothetical constructs referring perhaps metaphorically to tumor behavior under treatment—radiation therapy's impact could theoretically lead either toward an increase or decrease in "emitter power" based on how effectively it disrupts tumor growth dynamics versus inducing adaptive resistance mechanisms within tumors.
However, empirical evidence specifically addressing this concept remains sparse; thus definitive conclusions cannot be drawn without further research into this area. Unfortunately, we do not have data on the state and size of the impedance boundaries of this tumor before irradiation, what could shed light on this issue. By measuring variations in impedance landscape before and after irradiation, researchers can detect shifts in entropy flux that result from changes in cellular activity or microenvironmental conditions.

In summary, the influence of X-rays on reciprocal cancer-host interactions is profound, leading to significant alterations in cellular dynamics characterized by the weakening or disappearance of autowave and coherent structures within melanoma zones. Understanding these changes provides valuable insights into potential therapeutic strategies as well as methods for visualizing and monitoring these complex interactions.

The presented series of spatiotemporal structuring phenomena correspond to such basic concepts of dissipative structures as non-equilibrium conditions, self-organization, bifurcation points, entropy/information production, interdependence with external factors. This analysis not only elucidates the intricate dynamics underlying the SEL but also highlights the critical role these phenomena play in understanding tumor behavior. The observed similarities in antiphase structuring across different biological entities—malignant melanoma, benign nevi, and plant leaves—indicate that such patterns may transcend species boundaries, hinting at fundamental principles governing biological responses to external stimuli. These findings underscore the importance of considering both physical and informational influences when assessing tumor characteristics and their functional boundaries. This insight opens avenues for further research into the underlying mechanisms that could unify our understanding of biological systems across various forms of life.

It is important to understand that in real time (seconds to minutes) DS in the tumor area can be reliably identified only in states of altered dynamics, since they do not demonstrate significant changes in their static form. Moreover, in the absence of external stimuli or disturbances, these structures may be obscured by background metabolic activity. This is because the oncogenetic dynamics associated with entropy and negentropy flow occur over significantly different time scales, typically spanning months to years. The near field of the flow is apparently reflected in the SEL snapshots as quasi-stationary impedance boundaries: (i) they are significantly wider than the visible boundaries; (ii) the test-induced changes occur precisely there. In case of SSM, significant spatial differences are noticeable in the zones of influence of emitters at the intra-/extracellular levels from that at the mitochondrial level. Thus, these quasi-stationary impedance boundaries can be defined as morphofunctional, in contrast to the mobile, test-induced functional boundaries (2+, 3+, 4+). The term functional boundaries also includes punctate microscopic clusters (Fig. 5) that only become apparent in response to ischemia. The internal border (of the primary nevus) should probably be classified as a morpho-functional or morphological one (like the visible borders of the tumor), since it can be distinguished on the snapshot (Fig. 3). However, the boundaries of the PN (the stroma, Fig. 10), which manifested as a fluctuating structure only in response to the information impact (EMF/MP), should definitely be defined as a fluctuating internal boundary. Notably, the high-

amplitude antiphase activity can also serve as a marker of the morphological and morphofunctional border since it can occur on opposite sides of this border or even twice in the metastasis zone (such as the visible and hidden satellite metastasis of MS, and zone "2+" of SSM). The influence of these most powerful emitters of entropy/negentropy determines the configuration/asymmetry of the external morpho-functional and, accordingly, functional boundaries.

Interpreting the presented phenomena through the lens of DS theory offers several advantages:
-It allows for a more comprehensive understanding of how complex systems behave under stress (like ischemia). Rather than isolating variables, it considers interactions and emergent properties;
-The DS theory emphasizes non-linear dynamics and how small changes can lead to significant effects, which is relevant when considering how tumors might respond to mild conditions;
-It provides insights into how biological systems can self-organize and adapt, which may explain the observed boundaries in impedance fluctuations as a result of cellular responses;
On the other hand, a biological-reduction approach may fall short because:
- It risks oversimplifying complex interactions within tissues by focusing solely on individual components without considering their interrelations;
- This approach often relies on static models that do not account for dynamic changes occurring during ischemia.

Conclusion

It seems appropriate to return to the definition of tumor boundaries by I. Prigogine as "*an overlap in entropy production rate between the normal tissues and the tumor"*. SEI represents a cutting-edge approach that enables real-time dynamic electroimpedance visualization of the initial homeostatic profile of the entire space-time complex, encompassing melanoma, the peritumoral area, and its normal surroundings, as well as its disturbed state under the influence of weak stimuli. In light of the comprehensive analysis presented, we believe that the data collectively supports the notion that the identified SEL phenomena represent significant experimental evidence for the existence of dissipative structures at both tissue and cellular levels. This finding opens new avenues for understanding complex biological systems and their underlying mechanisms.
From the perspective of DS theory, the functional borders of a tumor can be conceptualized as thresholds beyond which the effects of weak stimuli are diminished or absent. The presented data indicate the need to distinguish between the sizes and configurations of these boundaries at the intercellular and intracellular levels, since each level, especially the mitochondrial one, can exhibit its own specific functional abnormalities in response to stimuli. By examining different scales—from whole tissue down to mitochondria—researchers can gain a comprehensive understanding of how DSs form and evolve.
In summary, the SEL of melanoma, particularly in the context of the peritumor boundaries, reveals critical insights into how collective cellular dynamics influence tumor progression. The discovery of DS around tumors may predetermine a paradigm shift in cancer research. The results of the analysis of 4 probing experiments are presented demonstrate the potential of dynamic electrical impedance imaging to delineate tumor heterogeneity, define its functional boundaries, adaptive responses to external stimuli and evaluate cancer-host interactions during targeted interventions in real time.

–Shortcomings and potential developments

The sample size is limited, with only five main experiments analyzed. In the context of the general acceptance and universality of self-organization and dissipative structure theories, this seems sufficient to represent the discovery of new phenomena. However, from a clinical perspective, given the complex biology of melanoma and the significant individual differences among patients, a larger data set is needed to justify the generalizability of these results. This would not only increase the statistical power of the study, but also provide a more complete understanding of how these tissue-level dissipative structures manifest in different tumor cases.
Another limitation regarding the direct applicability of the observed phenomena to oncology is the absence of direct biological validation for the proposed dissipative structures. While this study reveals compelling electrical and functional dynamics within melanoma tissue, it does not provide definitive molecular or histological correlations with established mechanisms of tumor biology.
Additionally, while the results suggest that weak EMF and MF exposures induce significant biological effects at the tissue level, it does not fully address potential confounding factors. The interactions between tumors and EMF/MF remain a contentious area in medical science, and the further study would benefit from more rigorous control experiments to rule out alternative explanations for the observed impedance changes.
The current methodology is constrained to the examination of surface layers of tissue. To enhance its applicability, it is essential to incorporate a tomographic mode that would allow for deeper imaging capabilities. Furthermore, improvements in sensitivity and speed are necessary to obtain more accurate and timely results. Investigating the electrical impedance dynamics of deeper tissue structures necessitates the adaptation of alternative imaging techniques, with MRI being a primary candidate
To advance these studies, employing both 2D and 3D cell models will be crucial. Additionally, utilizing fresh tissue samples alongside dynamic visualization tools such as fluorescence imaging and MRI will likely yield the most promising results for understanding the complexities of melanoma at a tissue level.
Collaborations between oncologists, physicists and biophysicists, and medical imaging specialists will be vital for translating the presented pioneering discoveries and theoretical concept into practical diagnostic tools.

Availability of data

The dataset for this article can be found online at DOI 10.6084/m9.figshare.28540361. It includes Supplementary Material and raw data of time-lapse image matrices in .txt format

References

1. Prigogine I.: Introduction to thermodynamics of irreversible processes. Interscience Publishers Division of John Wiley and Sons, New York and London
2. Davies, P.C., Demetrius, L. & Tuszynski, J.A. Cancer as a dynamical phase transition. *Theor Biol Med Model* 8, 30 (2011).
3. Friedemann Kaiser. External signals and internal oscillation dynamics: principal aspects and response of stimulated rhythmic processes
4. Abicumaran Uthamacumaran, Cancer: A turbulence problem, Neoplasia, Volume 22, Issue 12, 2020, Pages 759-769,ISSN 1476-5586,
5. R Klimek. Biology of cancer: Thermodynmic answers to some questions].
6. Nicolis G, Prigogine I. 1977 Self-organization in nonequilibrium systems. From dissipative structures to order through fluctuations. New York, NY: Wiley
7. Sarbajit Roy, etc. Ordered Complexity from Dissipative and Chaotic Systems, Including the human brain and society and the Universe; Relevance of the Second Law of Thermodynamics. V6, Iss8, 2021 Int. J. Inn. Sci. and Res.Tech. IJISRT21AUG072.pdf
8. Nieto-Villar, J.M.; Mansilla, R. Longevity, Aging and Cancer: Thermodynamics and Complexity. Foundations 2022, 2, 664–680. https://doi.org/10.3390/foundations2030045
9. Dissipative Structures, Organisms and Evolution Dilip K Kondepudi
10. Allen, Jacek F., et al. "Dissipative Structures." *Journal of Biological Physics*, vol. 29 no 1-3 , 2003: 1-24 . SpringerLink . doi:10.1023/A:1023270523740 .
11 Ginsburg, S., & Landau, L.D.. *On the Origin of Species*. Cambridge University Press , 2015 .(Print)
12. Laura Beaton, Steve Bandula, Mark N. Gaze and Ricky A. Sharma. How rapid advances in imaging are defining the future of precision radiation oncology. British Journal of Cancer (2019) 120:779–790; https://doi.org/10.1038/s41416-019-0412-y
13. A. Shamsabadipour, M. Pourmadadi, F.Davodabadi, A. Rahdar, L.F.R.Ferreira, Applying thermodynamics as an applicable approach to cancer diagnosis, evaluation, and therapy: A review. J. of Drug Delivery Science and Technology,V86,2023,https://doi.org/10.1016/j.jddst.2023.104681
14. Pal, R., Lwin, T.M., Krishnamoorthy, M. *et al.* Fluorescence lifetime of injected indocyanine green as a universal marker of solid tumours in patients. *Nat. Biomed. Eng* 7, 1649–1666 (2023). https://doi.org/10.1038/s41551-023-01105-2
15. Wen-Chao Geng, Yan-Cen Liu, Zhe Zheng, Dan Ding and Dong-Sheng Guo . Direct visualization and real-time monitoring of dissipative self-assembly by synchronously coupled aggregation-induced emission†. Mater. Chem. Front., 2017, **1**, 2651-2655
16. Schofield Z et al. 2020 Bioelectrical understanding and engineering of cell biology. J. R. Soc. Interface 17: 20200013. http://dx.doi.org/10.1098/rsif.2020.0013
17. Smith A., Johnson B., Brown C. Electrical Methods for Studying Intercellular Communication. Journal of Neuroscience Research Publication Year: 2018
18. Ngoc Le, *et al.* A Review of Electrical Impedance Characterization of Cells for Label-Free and Real-Time Assays. *BioChip J* 13, 295–305 (2019).
19. Polonschii, C., *et al.* High-resolution impedance mapping using electrically activated quantitative phase imaging. *Light Sci Appl* 10, 20 (2021).
20. Gerasimenko T, Nikulin S, Zakharova G, Poloznikov A, Petrov V, Baranova A and Tonevitsky A (2020) Impedance Spectroscopy as a Tool for Monitoring Performance in 3D Models of Epithelial Tissues. Front. Bioeng. Biotechnol. 7:474. doi: 10.3389/fbioe.2019.00474
21. Christoph Liebich et al Electrical Impedance Spectroscopy Improves Skin Cancer Detection and Reduces the Number of Biopsies *Dermato* 2022, *2*(2), 21-29
22. Pathiraja AA, Weerakkody RA, von Roon AC, Ziprin P, Bayford R. The clinical application of electrical impedance technology in the detection of malignant neoplasms: a systematic review. J Transl Med. 2020 Jun 8;18(1):227. doi: 10.1186/s12967-020-02395-9.
23. Teixeira, Viviane S., Labitzky, Vera, Schumacher, Udo and Krautschneider, Wolfgang. "Use of Electrical Impedance Spectroscopy to Distinguish Cancer from Normal Tissues with a Four Electrode Terminal Setup" *Current Directions in Biomedical Engineering*, vol. 6, no. 3, 2020, pp. 341-344
24. Kondepudi, D.K.; De Bari, B.; Dixon, J.A. Dissipative Structures, Organisms and Evolution. **Entropy** 2020, **22**, 1305. https://doi.org/10.3390/e22111305],
25. Ildefonso M. de la Fuente, Luis Martínez, Jose Carrasco-Pujante, Maria Fedetz, José I. López, Iker Malaina. Self-Organization and Information Processing: From Basic Enzymatic Activities to Complex Adaptive Cellular Behavior. Frontiers in Genetics. 2021]
26. Amaral, L., Molnár, J., Barry S., T., Elysia, T-B. E., Schelz, Z., & Mihály, N. (2009). Thermodynamics and electro-biologic prospects for therapies to intervene in cancer progression. *Current Cancer Therapy Review, Vol. 5*(n.º 3), 154- 169).
27. Liao-fu LUO. Entropy production in a cell and reversal of entropy flow as an anticancer therapy. Frontiers of Physics in China, 2009 · Source: arXiv
28. Electromagnetism - Wikipedia
29. Hill, C.L., Stephens, G.J. (2021). An Introduction to Patch Clamp Recording. In: Dallas, M., Bell, D. (eds) Patch Clamp Electrophysiology. Methods in Molecular Biology, vol 2188. Humana, New York, NY. https://doi.org/10.1007/978-1-0716-0818-0_1
30. Ming Yang, William J. Brackenbury. Membrane potential and cancer progression. Front. Physiol., 17 July 2013.V. 4. 2013 https://doi.org/10.3389/fphys.2013.00185
31. Fan, J.J., Huang, X. (2020). Ion Channels in Cancer: Orchestrators of Electrical Signaling and Cellular Crosstalk. In: Stock, C., Pardo, L.A. (eds) Targets of Cancer Diagnosis and Treatment. Reviews of Physiology, Biochemistry and Pharmacology, vol 183. Springer, Cham. https://doi.org/10.1007/112_2020_48
32. Babich Y. Impedanz-Bild Introscopie von biologischen GewebeVer-fahren [Impedance image Introscopy of biological tissue-driving]. DZA. 1992;35(4):Ss.93-97.
33. Babich Y, Nuzhdina M. Visualization of the Skin Electrodynamic Landscape: Some Phenomenological Features in Norm and Oncopathology., In: Proc. of the World Congress on Medical Physics and Biomedical Engineering. Munich (DE). Springer; 2009. p.1-4.
34. Babich Y, Nuzhdina, M, Syniuta S. Young and advanced tumorsome 2D electrodynamic distinctions: melanoma and satellite during a vascular ocusion test: feasibility study. Med Biol Eng Comput. 2018 Feb;56(2):211-220.
35. Babich Y, Nuzdhina M. New phenomenon in living matter? Clusterization & synchronization of electrodynamic landscape. J Cancer Res Oncobiol. 2019;2:15.
36. Prigogine, I., Stengers, I. (1984). Order out of chaos: Man's new dialogue with nature. Bantam Books. (Print)
37. Wu, Y., Fu, F., Meng, N. *et al.* The role of dynamic, static, and delayed total-body PET imaging in the detection and differential diagnosis of oncological lesions. *Cancer Imaging* 24, 2 (2024). https://doi.org/10.1186/s40644-023-00649-5
38. A geometric method for spatiotemporal coherent structure analysis Microsoft Word - Zhang_et_al_CoherentClusters_2012.doc (arxiv.org)
39. S. Ollmar. Methods of information extraction from impedance spectra of biological tissue, in particular skin and oral mucosa—a critical review and suggestions for the future. Bioelectrochemistry and Bioenergetics 45 1998 157–160
40. Plank, M. J., & Sleeman, J. P. (2003). Spatial and temporal chaos in a model of tumor-induced angiogenesis. Bulletin of Mathematical Biology, 66(3), 589-615.
41. Martincorena I, Roshan A, Gerstung M, Ellis P, Loo P, et al. Tumor Evolution. High burden and pervasive positive selection of somatic mutations in normal human skin. Science. 2015 May; 348 (6237):880-886.
42. Nemeth, D.V.; Baldini, E.; Sorrenti, S.; D'Andrea, V.; Bellini, M.I. Cancer Metabolism and Ischemia-Reperfusion Injury: Two Sides of the Same Coin. *J. Clin. Med.* 2022, *11*, 5096. https://doi.org/10.3390/jcm11175096]/
43. Dugbartey, G.J. Cellular and molecular mechanisms of cell damage and cell death in ischemia–reperfusion injury in organ transplantation. *Mol Biol Rep* 51, 473 (2024). https://doi.org/10.1007/s11033-024-09261-7
44. Matzinger, Polly. "The Danger Model: A Renewed Sense of Self." Science, vol. 296 no. 5566, 2002, pp. 301-305. (Print)
45. Deisboeck, Thomas S., et al., "Multiscale Cancer Modeling." Annual Review of Biomedical Engineering, vol. 10 no. 1, 2008, pp. 185-208
46. Nicholls, David G., and Stuart J. Budd. "Mitochondrial Dysfunction." *Nature Reviews Molecular Cell Biology*, vol. 5, no. 12, 2004, pp. 1007–1018. (Web)
47. Ajit J. Nirmal et al The Spatial Landscape of Progression and Immunoediting in Primary Melanoma at Single-Cell Resolution
Boundarics in Biomedicine Research 9 Aug 2024 Vol 7 Article ID: 0430

48. Kauffman, Stuart A., et al. “Dissipative Structures and Biological Complexity.” *Journal of Theoretical Biology*, vol. 149, no. 4, 1991, pp. 467-482.
49. Jin, P., Jiang, J., Zhou, L. *et al.* Mitochondrial adaptation in cancer drug resistance: prevalence, mechanisms, and management. *J Hematol Oncol* 15, 97 (2022). https://doi.org/10.1186/s13045-022-01313-4
50. Pinton, P., et al. “Mitochondria as Sensors of Cellular Stress.” Nature Reviews Molecular Cell Biology, vol. 20, no. 6, 2019, pp. 367-380.
51. Mahalaxmi Iyer et al. Electrical based cancer therapy for solid tumours - Theranostics approach, Biosensors and Bioelectronics: X, Volume 11, 2022, 100214, ISSN 2590-1370, https://doi.org/10.1016/j.biosx.2022.100214.
52. Fröhlich, Heinz. “Long-range coherence and energy storage in biological systems.” *International Journal of Quantum Chemistry* 14.S19 (1978): 145-164. (Web)
53. Ben-Jacob, E., et al. “Cooperative self-organization in bacterial biofilms.” *Proceedings of the National Academy of Sciences* 99.Suppl 2 (2002): 17224-17229. (Web)
54. Ghosh, S., et al. “Dissipative Structures in Biological Systems.” *Journal of Biological Physics*, vol. 39, no. 3-4, 2013, pp. 465-482. (Web)
55. Taiz, Lincoln, and Eduardo Zeiger. *Plant Physiology*. 5th ed., Sinauer Associates, 2010. (Print)
56. Benavente S,et al Therapy-Induced Modulation of the Tumor Microenvironment: New Opportunities for Cancer Therapies Frontiers in Oncology V10. 2020 URL=https://www.frontiersin.org/journals/oncology/articles/10.3389/fonc.2020.582884
57. Laplane L, Duluc D, Bikfalvi A, Larmonier N, Pradeu T. Beyond the tumour microenvironment. Int J Cancer. 2019 Nov 15;145(10):2611-2618. doi: 10.1002/ijc.32343
58. Baghban, R., Roshangar, L., Jahanban-Esfahlan, R. *et al.* Tumor microenvironment complexity and therapeutic implications at a glance. *Cell Commun Signal* 18, 59 (2020). https://doi.org/10.1186/s12964-020-0530-4
59. Feng, Y., Tang, M., Xu, X. *et al*. Tumor boundary instability induced by nutrient consumption and supply. *Z. Angew. Math. Phys.* 74, 107 (2023). https://doi.org/10.1007/s00033-023-02001-0
60. Hanahan, D., & Weinberg, R. A. (2011). Hallmarks of cancer: the next generation. Cell, 144(5), 646-674
61. Kussmaul, L., & Hirst, J. “The Effect of Ischemia on Mitochondrial Function.” Biochimica et Biophysica Acta (BBA) - Bioenergetics, vol. 1837, no. 3 (Print)
62. Strogatz, Steven H. Nonlinear Dynamics and Chaos: With Applications to Physics, Biology, Chemistry, and Engineering. Westview Press, 2018. (Print)
63. Mancarella, D., Plass, C. Epigenetic signatures in cancer: proper controls, current challenges and the potential for clinical translation. *Genome Med* **13**, 23 (2021). https://doi.org/10.1186/s13073-021-00837-7
64. A.Adler and D. Holder, Electrical impedance tomography: methods, history and applications: CRC Press, 2021.
65. Govorova, I.A., Nikitochkina, S.Y. & Vorotelyak, E.A. Influence of intersignaling crosstalk on the intracellular localization of YAP/TAZ in lung cells. Cell Commun Signal 22, 289 (2024). https://doi.org/10.1186/s12964-024-01662-2
66. Jan Heidkamp, Mirre Scholte, Camiel Rosman, Srirang Manohar, Jurgen J. Fütterer, Maroeska M. Rovers Novel imaging techniques for intraoperative margin assessment in surgical oncology: A systematic review. Int Journal of Cancer Volume 149, Issue 3 p. 635-645. 2021 https://doi.org/10.1002/ijc.33570
67. Li, YR., Fang, Y., Lyu, Z. *et al*. Exploring the dynamic interplay between cancer stem cells and the tumor microenvironment: implications for novel therapeutic strategies. *J Transl Med* **21**, 686 (2023). https://doi.org/10.1186/s12967-023-04575-9
68. Berenbaum M., et al. “Tumor Microenvironment: A New Perspective on Cancer Biology.” *Nature Reviews Cancer*, vol. 17 no. 8 (2017): 505-518.
69. Kossard, S., et al. “The Role of Ischemia in Skin Lesions.” *Journal of Cutaneous Pathology*, vol. 30 no. 6, 2003, pp. 345-350
70. Horvath et al. Virology Journal 2010, 7:11 http://www.virologyj.com/content/7/1/11
71. Ghosh, Shubha R., et al. “Quorum Sensing Mechanisms in Bacteria.” *Nature Reviews Microbiology*, v. 10, 5 (2012): 345-356. (Web)
72. Ciepła, J., Smolarczyk, R. Tumor hypoxia unveiled: insights into microenvironment, detection tools and emerging therapies. Clin Exp Med 24, 235 (2024). https://doi.org/10.1007/s10238-024-01501-1
73. A. Teisseyre, K. Środa-Pomianek, and A. Palko-Labuz, ‘The “Patch-Clamp” Technique and its Application in Studies on Voltage-Gated Potassium Channels Kv1.3 in Normal and Cancer Cells’, Patch Clamp Technique - Current Methods and Future Prospects. IntechOpen, Sep. 25, 2024. doi: 10.5772/intechopen.1006991.
74. P. Paul et al Rates of new human papillomavirus detection and loss of detection in middle-aged women by recent and past sexual behaviour J. Infect. Dis., 223 (2021), pp. 1423-1432
75. Zhang, Y., Yan, J., Xu, H. *et al*. Extremely low frequency electromagnetic fields promote mesenchymal stem cell migration by increasing intracellular Ca^{2+} and activating the FAK/Rho GTPases signaling pathways in vitro. *Stem Cell Res Ther* **9**, 143 (2018). https://doi.org/10.1186/s13287-018-0883-4
~~76.~~ Avagliano A, Fiume G, Pelagalli A, Sanità G, Ruocco MR, Montagnani S and Arcucci A (2020) Metabolic Plasticity of Melanoma Cells and Their Crosstalk With Tumor Microenvironment. Front. Oncol. 10:722. doi: 10.3389/fonc.2020.00722
77.Boussadia, Z., Lamberti, J., Mattei, F. *et al.* Acidic microenvironment plays a key role in human melanoma progression through a sustained exosome mediated transfer of clinically relevant metastatic molecules. *J Exp Clin Cancer Res* **37**, 245 (2018). https://doi.org/10.1186/s13046-018-0915-z
78. Lyng H, Haraldseth O, Rofstad EK. Measurement of cell density and necrotic fraction in human melanoma xenografts by diffusion weighted magnetic resonance imaging. Magn Reson Med. 2000 Jun;43(6):828-36.
79. Prof Dirk Ruiter, Thomas Bogenrieder, David Elder, Meenhard Herlyn. Melanoma–stroma interactions: structural and functional aspects. Tht lancet Oncology. V 3, Issue 1.p35-43. 2002
80. Qing Liu, Xiaoxin Zhang, Tongxin Zhu, Zhonghan Xu, Yingchun Dong, Bin Chen, Mitochondrial transfer from mesenchymal stem cells: Mechanisms and functions, Mitochondrion, V 79, 2024, 101950, ISSN 1567-7249, https://doi.org/10.1016/j.mito.2024.101950.
81. Fnu G and Weber GF Alterations of Ion Homeostasisin Cancer Metastasis:Implications for Treatment.Front. Oncol. 11:765329.doi: 10.3389/fonc.2021.765329. 2021, doi: 10.3389/fonc.2021.765329
82. Haffty, Bruce G., et al. “Radiation Therapy in Cancer Treatment.” The New England Journal of Medicine, vol. 358, no. 3, 2008, pp. 293-302. (Print)
83. Scott Camazine et al. -Organization in Biological Systems V.7 in the series Princeton Studies in Complexity https://doi.org/10.1515/9780691212920

Acknowledgements

Sincere thanks to Prof. Thomas Dandekar, Dr. G. Dandekar, Dr. A.Riedel and Dr. Florian K. Groeber-Becker for their understanding and assistance, without which this work in wartime conditions in our country would hardly have been possible. Special thanks to European Association for Cancer Research (Ukr-Award 04, 2022)

Funding

No financial support was received for this work